iScience

Article
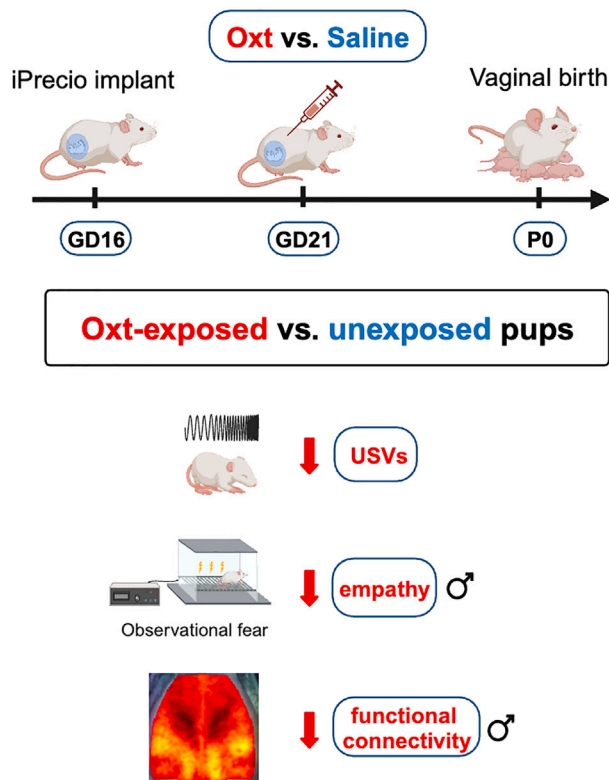
Oxytocin-induced birth causes sex-specific behavioral and brain connectivity changes in developing rat offspring

Oxt-induced labor alters offspring behavior and brain connectivity

iPrecio implant — Oxt vs. Saline — Vaginal birth

GD16 — GD21 — P0

Oxt-exposed vs. unexposed pups

↓ USVs

↓ empathy ♂
Observational fear

↓ functional connectivity ♂

Tusar Giri, Susan E. Maloney, Saswat Giri, ..., James D. Quirk, Adam Q. Bauer, Arvind Palanisamy

arvind.palanisamy@wustl.edu

Highlights
Induced birth with oxytocin did not affect maternal and neonatal wellbeing

Maternally administered oxytocin downregulated oxytocin receptor in the developing brain

Oxytocin exposure at birth altered early life communication in the pups

Oxytocin exposed offspring had sex-specific deficits in empathy and brain connectivity

Article

Oxytocin-induced birth causes sex-specific behavioral and brain connectivity changes in developing rat offspring

Tusar Giri,[1] Susan E. Maloney,[2] Saswat Giri,[3] Young Ah Goo,[4,5] Jong Hee Song,[5] Minsoo Son,[5] Eric Tycksen,[6] Sara B. Conyers,[2] Annie Bice,[7] Xia Ge,[7] Joel R. Garbow,[7] James D. Quirk,[7] Adam Q. Bauer,[7] and Arvind Palanisamy[1,8,9,*]

SUMMARY

Despite six decades of the use of exogenous oxytocin for management of labor, little is known about its effects on the developing brain. Motivated by controversial reports suggesting a link between oxytocin use during labor and autism spectrum disorders (ASDs), we employed our recently validated rat model for labor induction with oxytocin to address this important concern. Using a combination of molecular biological, behavioral, and neuroimaging assays, we show that induced birth with oxytocin leads to sex-specific disruption of oxytocinergic signaling in the developing brain, decreased communicative ability of pups, reduced empathy-like behaviors especially in male offspring, and widespread sex-dependent changes in functional cortical connectivity. Contrary to our hypothesis, social behavior, typically impaired in ASDs, was largely preserved. Collectively, our foundational studies provide nuanced insights into the neurodevelopmental impact of birth induction with oxytocin and set the stage for mechanistic investigations in animal models and prospective longitudinal clinical studies.

INTRODUCTION

Despite six decades of the use of exogenous oxytocin (Oxt) for induction and augmentation of labor,[1,2] one of the most common clinical interventions in obstetric practice, little is known about its effects on the developing brain. Epidemiological evidence, albeit conflicting, suggests a link between the use of Oxt and neurodevelopmental disorders. For example, labor induction and/or augmentation was associated with a 23% increased odds for autism diagnosis,[3] an increased risk for autism in males,[4] a 2-fold increased prevalence of abnormal autism-like behaviors in the offspring,[5,6] and reduced school performance in children at age 12.[7] Similarly, such practice has been linked to a 2.5-fold increased risk for impaired cognition, bipolar disorder, and attention deficit hyperactivity disorder in children.[8,9] These studies are counterbalanced by evidence that suggests a lack of impact of these practices on the incidence of neurodevelopmental disorders.[10–12] Nevertheless, epidemiological studies are inconclusive because of (i) wide variations in obstetric practice, (ii) lack of cumulative Oxt dose data, and more importantly, (iii) their inability to distinguish the need for labor induction from its effects and to separate the effect of Oxt from other drugs used during labor induction (e.g., prostaglandins). Recently, however, a case-control study reported for the first time, a dose-response relationship between Oxt use during labor and autism spectrum disorders (ASD). Specifically, male offspring exposed to either a higher cumulative dose of Oxt (odds ratio OR 2.8, 95% CI 1.1–7.7) or a longer duration of Oxt infusion (OR 3.5, 95% CI 1.3–9.4) had significantly higher odds of developing ASD.[13] For every 500 mIU increase in cumulative Oxt dose or 500 min increase in the duration of Oxt exposure, the odds for ASD diagnosis increased by 1.1 or 2.1, respectively, among boys. Notably, these associations were absent in the female offspring. Despite these recurring concerns, and evidence for Oxt transfer across the human placenta,[14,15] the mechanisms by which Oxt could impact the fetus remain unresolved.

Oxt infusion regimens were introduced in obstetrics many decades ago,[16–18] prior to the seminal discoveries that established the non-obstetric role of Oxt as a pivotal neurotransmitter. Oxt, acting through the Oxt receptor (Oxtr), is essential for the maturation of social behaviors during development, and is an important neurotransmitter for modulating trust, compassion, and empathy behaviors.[19–28] Despite

[1]Department of Anesthesiology, Washington University School of Medicine, St. Louis, MO, USA
[2]Department of Psychiatry, Intellectual and Developmental Disabilities Research Center, Washington University School of Medicine, St. Louis, MO, USA
[3]Graduate Student, School of Public Health and Social Justice, St. Louis University, St. Louis, MO, USA
[4]Department of Biochemistry and Molecular Biophysics, Washington University School of Medicine, St. Louis, MO, USA
[5]Mass Spectrometry Technology Access Center (MTAC), McDonnell Genome Institute, Washington University School of Medicine, St. Louis, MO, USA
[6]Genome Technology Access Center (GTAC), McDonnell Genome Institute, Washington University School of Medicine, St. Louis, MO, USA
[7]Mallinckrodt Institute of Radiology, Washington University School of Medicine, St. Louis, MO, USA
[8]Department of Obstetrics and Gynecology, Washington University School of Medicine, St. Louis, MO, USA
[9]Lead contact
*Correspondence: arvind.palanisamy@wustl.edu
https://doi.org/10.1016/j.isci.2024.108960

knowledge of these recently discovered critical roles of Oxt in human behavior, and evidence for transplacental transfer of maternally admin-istered Oxt,[14,29–31] a fundamental question still remains unanswered: can maternally administered Oxt affect oxytocinergic signaling in the developing brain? This lack of knowledge is concerning because Oxtr is a G-protein coupled receptor that is highly susceptible to desensi-tization and downregulation upon prolonged stimulation with Oxt,[32,33] such as during prolonged administration for the management of la-bor. Most studies on Oxt use focus solely on obstetric outcomes and immediate neonatal wellbeing without assessment of the long-term neurodevelopmental impact of such interventions.[27,28] Furthermore, given its ubiquitous use and the artificially elevated Oxt environment during the perinatal period (i.e., prophylactic use in postpartum hemorrhage), clinical studies with an Oxt-naive control group are challenging, if not impossible. Not surprisingly, there is a dearth of high quality evidence regarding neurodevelopmental health of children after induced birth with Oxt. This becomes even more concerning with the 15–20% rate of "elective" induction where labor is induced for provider or patient convenience.[34–37] Motivated by the urgent need for translational investigations, we developed and validated an innovative high-fidelity model for labor induction with Oxt that mimics management of labor in pregnant women.[38] By using an implantable and pre-programmable microprocessor-controlled infusion pump connected internally to the jugular vein, we circumvented the drawbacks of previous animal models, to allow for precise intravenous Oxt dose escalation over time to electively induce birth in term pregnant rats. In this report, we used this model to perform a series of experiments to test the hypothesis that elective labor induction with Oxt would disrupt the develop-mental expression of Oxtr and cause sex-specific abnormalities in social behavior of the offspring.

RESULTS

Birth induction with Oxt does not affect maternal nurturing and neonatal wellbeing

To assess whether birth induction with Oxt affects maternal and neonatal wellbeing, we performed a series of quantitative and semi-quali-tative experiments (Figure 1). Litter sizes and pup survival rates were comparable between Oxt-induced and spontaneous birth (Figures S1A and S1B). The latency to retrieve the first pup, the total time to retrieve all pups, and the overall efficacy of pup retrieval were comparable in Oxt-exposed and unexposed rats in the pup retrieval test (Figure 1A). Similarly, the overall proportion of time spent in maternal (licking/grooming, nest building and maintenance, active/passive nursing) and non-maternal behaviors (self-care, feeding, drink-ing) were comparable (Figures 1B, 1C, S1C, and S1D). These findings were additionally supported by the semi-quantitative licking and groom-ing "pen mark" assay showing lack of significant differences in maternal nurturing behavior (Figures 1D and 1E). Milk intake of both Oxt-exposed and unexposed pups, as measured by the weigh-suckle-weigh (WSW) method, was comparable (Figure 1F). Finally, the pre-weaning weight trajectories of both Oxt-exposed and unexposed pups were similar (Figure 1G). Collectively, our data indicated that birth induction with Oxt did not affect maternal nurturing or impact neonatal wellbeing.

Maternal Oxt undergoes placental transfer and affects Oxt signaling in the developing brain

To confirm placental transfer of Oxt during prolonged infusion during labor, we assayed Oxt levels in the maternal/fetal plasma, and the brains of pups delivered by cesarean section at gestational day (GD) 22 (schematic in Figure 2A). Overall, there was a significant increase in maternal plasma Oxt (Figure 2B), and an approximately 2-fold increase in Oxt in the fetal plasma (Figure 2C) and brain of Oxt-exposed pups (Figure 2D), suggesting that Oxt is capable of crossing both the placental and the fetal blood-brain barrier. Commercially available ELISA does not distinguish exogenous Oxt from endogenous oxytocin, such that it is challenging to calculate maternal-to-neonatal transfer ratio with precision. To address this, we infused custom-synthesized stable isotope labeled Oxt (SIL-Oxt) in the G21 dam with the same pro-tocol as that for Oxt (schematic in Figure 2E), and subsequently assayed for the presence of SIL-Oxt in maternal and simultaneously collected pooled neonatal blood with mass spectrometry (Figure 2F). We detected SIL-Oxt in the newborn plasma (Figure 2G), which was approxi-mately 0.1% of the maternal plasma SIL-Oxt concentration.

Because of evidence for placental transfer of Oxt, we focused on the direct effect of Oxt on Oxt-ergic signaling mechanisms in the devel-oping brain (Figure 2H). Prolonged exposure to Oxt is known to downregulate the Oxtr.[32,33,39] Therefore, we tested this possibility with qPCR (Figure 2I) and western blot (Figures 2J, 2K, and S2) and confirmed a substantial decrease in Oxtr expression in the developing GD22 fetal cortex of pups exposed to Oxt in utero. To test whether this effect could be dose-dependent, we compared the extent of Oxtr gene down-regulation at higher Oxt doses (2x and 4x) using fetal cortical samples collected at GD22 during our previous study.[38] We noted that Oxt dose-dependently decreased the expression of Oxtr gene (Figure 2L). Motivated by evidence for altered DNA methylation of the Oxtr promoter after Oxt treatment,[31] we tested this possibility and noted that birth induction with Oxt was associated with a substantial decrease in DNA methylation of the Oxtr promoter in the fetal cortex of Oxt-exposed offspring (Figures 2M and 2N). Finally, in a vaginal birth cohort, we tracked the trajectory of Oxtr expression immediately after birth. Consistent with Oxtr downregulation observed at GD22, cortical Oxtr expression was downregulated in P1 pups (Figure 2O). Taken together, our data suggested that maternally administered Oxt during labor induction can reach the neonatal circulation and influence Oxtr regulation in the developing brain.

Oxt-induced birth causes communicative delay and sex-specific deficits in empathy behavior

In a separate set of experiments, we assayed Oxt-exposed and unexposed male and female pups in a series of behavioral tasks to assess early communicative behavior (pre-weaning period), and social communication, anxiety-like behaviors, behavioral flexibility, sensorimotor gating, social approach, and empathy-like behaviors (in the juvenile offspring) (schematic of timeline of behavioral assessments in Figure 3A). Assess-ment of ultrasonic vocalizations (USV), a measure of early communicative behavior, at P8 revealed an overall decrease in the number of USV
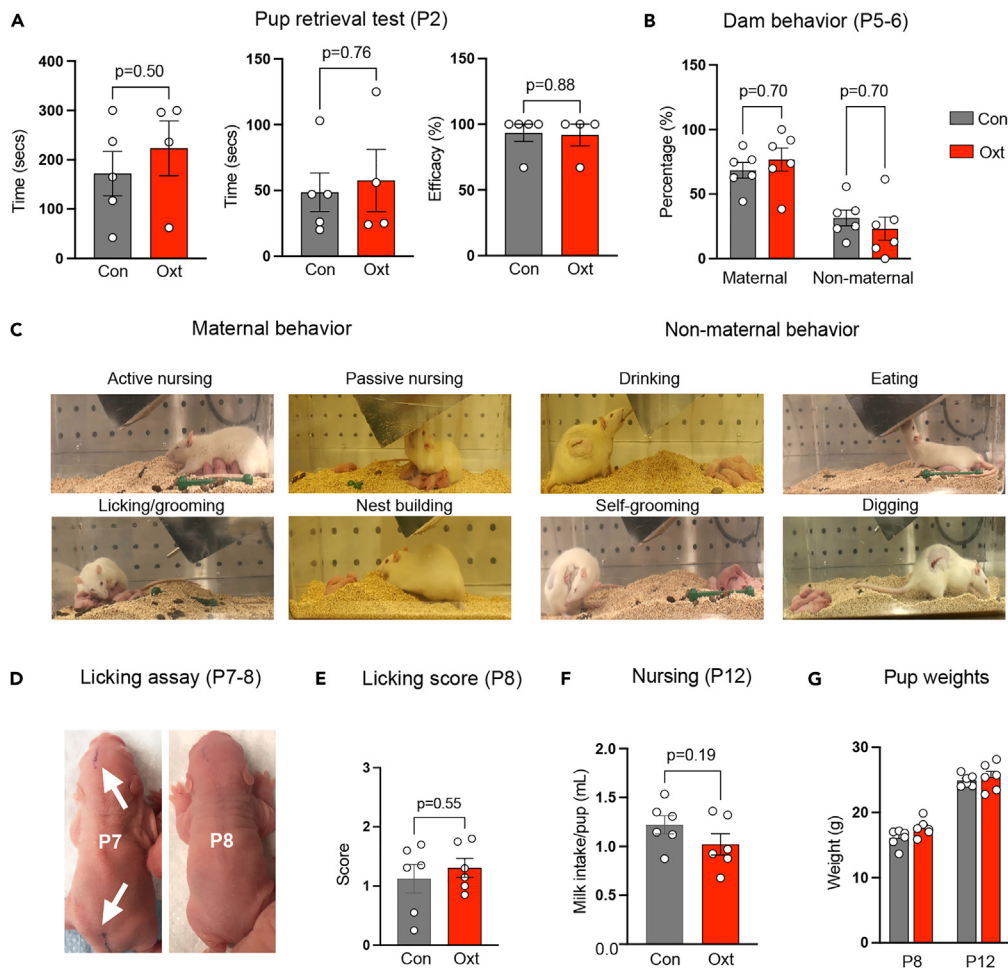
Figure 1. Impact of induced birth with oxytocin on maternal care and neonatal wellbeing

(A) Dot plots with bar graphs of the time to retrieve isolated pups and the latency and efficacy of pup retrieval. There were no differences between dams that spontaneously labored and dams whose labor was induced with Oxt.

(B) Dot plots with bar graphs showing that the proportion of maternal and non-maternal behaviors were no different between spontaneously laboring dams and dams whose labor was induced with Oxt.

(C) Representative photographs of maternal and non-maternal behavior.

(D) Representative photographs of a "marked" pup at P7 (white arrows at the back of the head and lower body close to the tail) and the "licked and groomed" pup 24 h later at P8.

(E) Dot plots with bar graphs of licking/grooming scores showing no differences in maternal care between unexposed and Oxt-exposed mothers.

(F) Dot plots with bar graphs of showing no differences in milk intake between unexposed and Oxt-exposed pups.

(G) Dot plots with bar graphs of pup weights at P8 and P12 showing no differences between unexposed and Oxt-exposed pups. Each data point represents a dam and/or its litter (n = 4–7 per condition). Data were analyzed with Welch's t-test and expressed as mean $\pm$ SEM.

calls and phrases in both Oxt-exposed male and female offspring (Figures 3B and S3A–S3E). The frequency of social interaction and social preference (Figures 3C, 3D, S3F, and S3G) behavior was no different between the groups, nor were there significant differences in social play behavior and juvenile dyadic USVs (Figures S3H–S3J). There were no observable differences in anxiety-like behaviors (i.e., no changes were noted in the proportion of time spent in the open vs. closed arms of the elevated plus maze) (Figures S3K and S3L), behavioral inflexibility tested with spontaneous alternation behavior in the Y-maze (Figure S3M), or the magnitude of prepulse inhibition of the startle reflex (Figures S3N and S3O). In the observational fear learning (OFL) task designed to assess empathy-associated behaviors, we noted a significant decrease in the percentage of freezing in male but not female Oxt-exposed pups when a sex-matched conspecific was shocked. Because freezing response is suggestive of emotional contagion and empathy-like behavior, a reduction in freezing response indicated the possibility of reduced empathy-like behavior in Oxt-exposed male pups (Figures 3E and S3P). These behavioral changes were not accompanied by differences in Oxtr expression in the medial prefrontal cortex (mPFC) (Figure 3F) and basolateral amygdala (BLA) of P40 offspring (Figure 3G), plasma Oxt levels (Figure 3H), and were not because of altered onset of puberty (Figures S4A–S4G). The constellation of behavioral findings
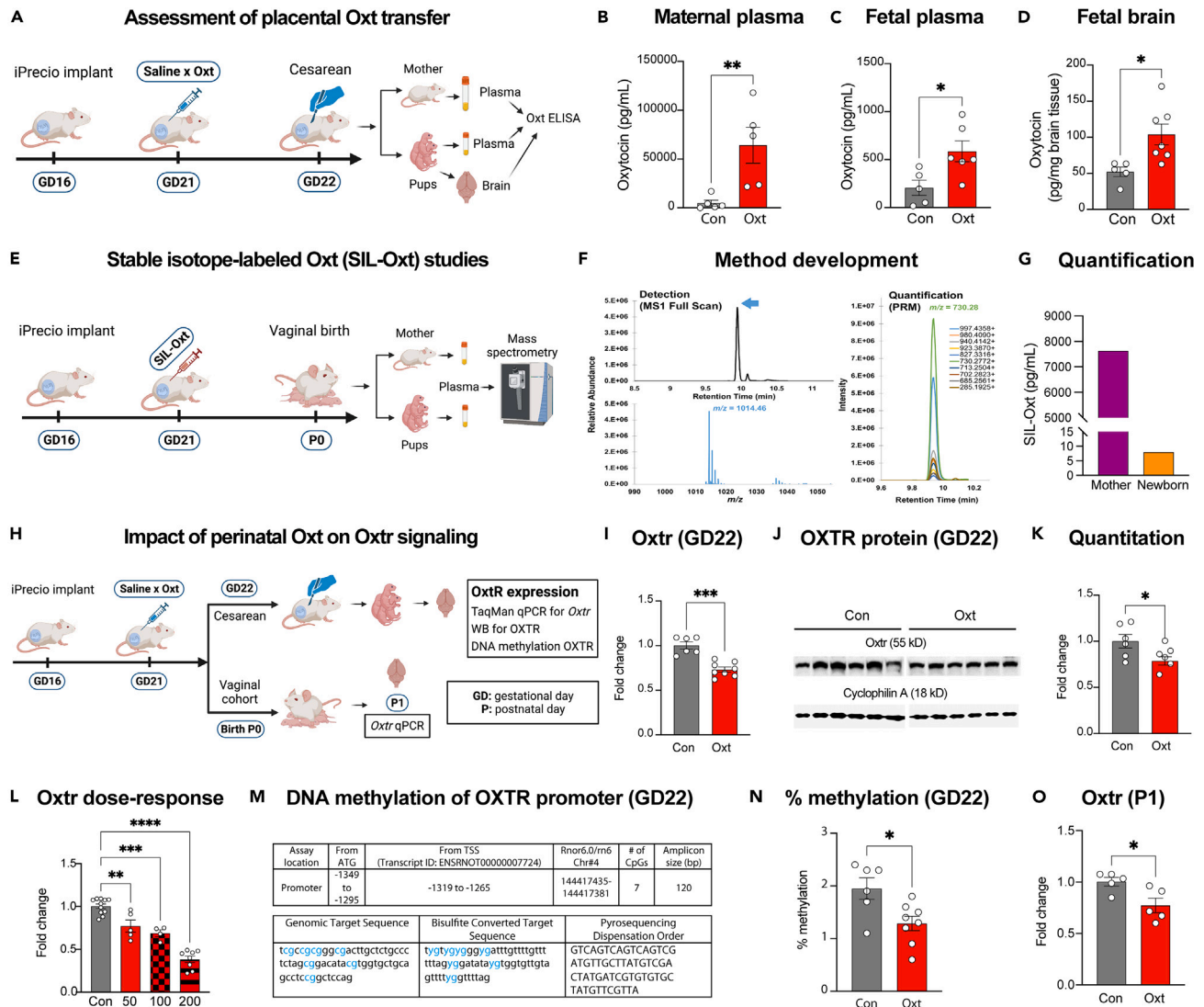
Figure 2. Assessment of placental transfer of Oxt and its impact on Oxtr in the developing brain

(A) Schematic for placental Oxt transfer experiments.

(B–D) Dot plots with bar graphs showing Oxt concentration in the maternal plasma, fetal plasma, and the fetal brain, respectively, showing a nearly 2-fold elevation of Oxt in the fetal plasma and brain after Oxt infusion.

(E) Schematic for stable isotope labeled Oxt (SIL-Oxt) experiments.

(F) Retention time and precursor ion, 1014.46 *m/z*, of SIL-Oxt and the PRM (parallel reaction monitoring) transitions. The topmost intense fragment ion, 730.28 *m/z*, was selected.

(G) Bar graph showing the presence of maternally administered SIL-Oxt in the newborn circulation confirming transplacental transfer of Oxt.

(H) Schematic of the experimental timeline for impact of Oxt on Oxtr in the developing brain.

(I) Dot plots with bar graphs showing a significant decrease in Oxtr gene expression in the fetal cortex.

(J) Immunoblots showing a decrease in the expression of OXTR protein in the fetal brain after maternal Oxt infusion. Lanes were run on the same gel but were non-contiguous.

(K) Dot plots with bar graphs showing densitometric quantification of the decrease in OXTR expression.

(L) Dot plots with bar graphs showing a dose-dependent decrease in Oxtr gene expression in the fetal cortex suggesting that the consequences for the fetus could be dependent on maternal Oxt dose.

(M) Details of the DNA methylation assay for the Oxtr.

(N) Oxt exposure was associated with a significant decrease in the % methylation of selected CpG sites in the Oxtr promoter region.

(O) Dot plots with bar graphs showing a decrease in Oxtr gene expression in the cortex of 1-day old vaginally born pups. Each data point represents a dam and/or its litter (n = 5–8 per condition except SIL-Oxt experiments). Data were analyzed with Welch's t-test or one-way ANOVA and expressed as mean ± SEM; *p < 0.05, **p < 0.01, ***p < 0.001, and ****p < 0.0001.
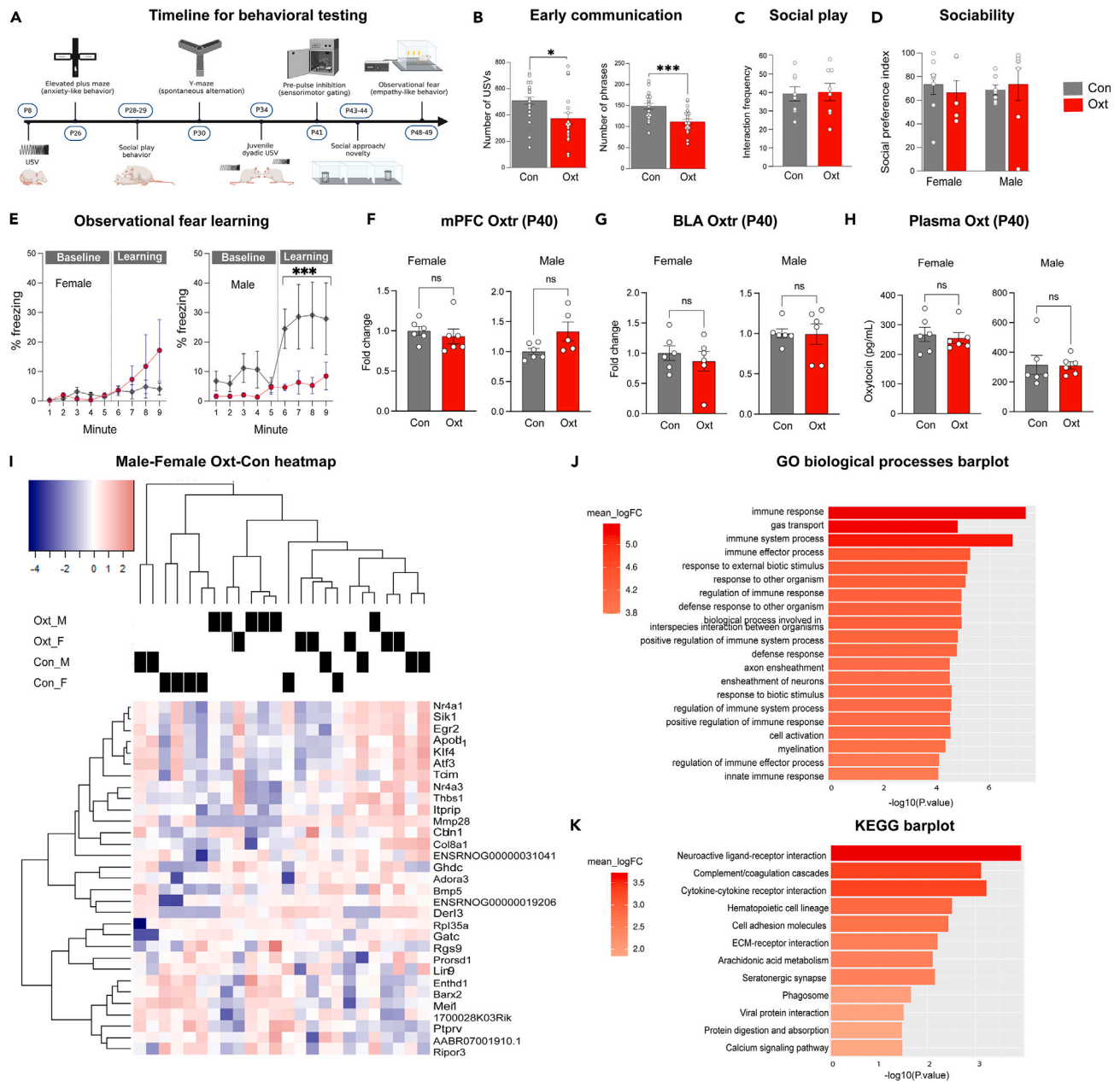
Figure 3. Neurobehavioral and transcriptomic changes in the offspring after induced birth with Oxt

(A) Schematic of the timeline of behavioral experiments from P8-P49.

(B) Reduced number of ultrasonic vocalizations (USV) and phrases in Oxt-exposed P8 offspring.

(C) Frequency of interaction during social play was not different after Oxt exposure.

(D) Social investigation, shown as social preference index, was largely preserved in both female and male offspring after Oxt-induced birth.

(E) Despite comparable freezing response at baseline, Oxt-exposed male pups displayed a significantly diminished freezing response during observational fear testing. Oxtr gene expression in the mPFC (F) and the BLA (G) was unaltered after Oxt exposure in both female and male P40 offspring.

(H) Plasma Oxt was no different in the P40 offspring whose birth was induced.

(I) Heatmap showing differentially expressed genes in male and female Oxt-exposed offspring, with sex of the offspring being the most important source of variation. Top 25 FDR-significant genes for gene ontology (GO) biological processes (J) suggesting upregulation of immune/inflammatory pathways.

(K) Significantly differentially expressed gene pathways identified with KEGG (Kyoto Encyclopedia of Genes and Genomes) analyses. Behavioral and assay data are expressed as mean $\pm$ SEM (n = 4–8 per treatment condition per sex, except Figure 3B where n = 16 per treatment condition with sexes combined); *p < 0.05, and ***p < 0.001. RNA-seq data were analyzed with Limma generalized linear models and GAGE as described (n = 6 per sex per treatment condition).
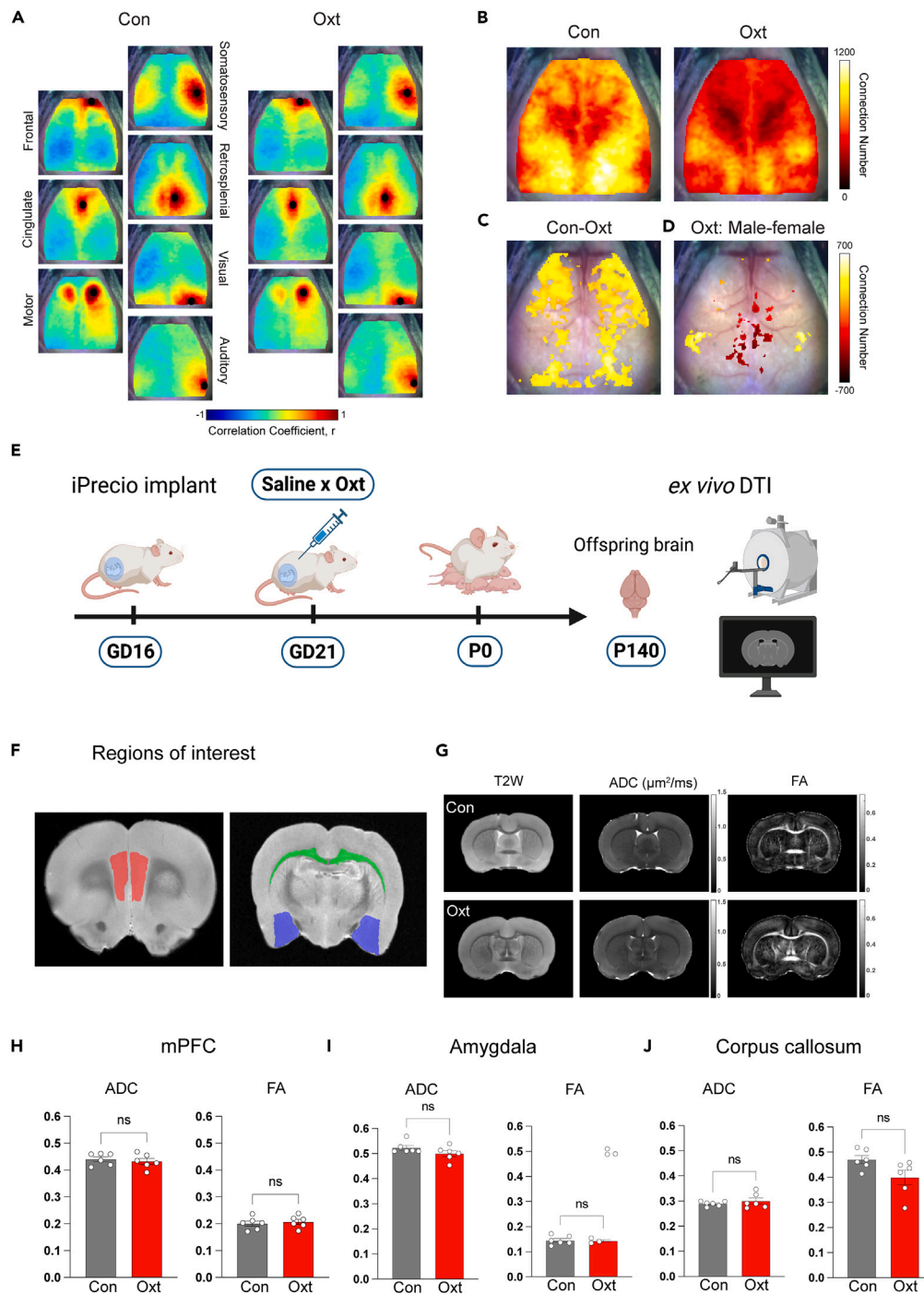
Figure 4. Electively induced labor with Oxt impairs functional brain connectivity in the developing brain

(A) Group averaged maps of functional connectivity seeds in cortical areas show a qualitative reduction in ipsilateral and bilateral connections in Oxt-exposed offspring (Oxt; right panel) primarily in frontal, motor, somatosensory, and visual regions.

(B) Control rats (Con; left panel) exhibited high connection number (yellows, whites) while Oxt-exposed rats (Oxt; right panel) exhibited more global reductions in node degree (reds). Main group-wise differences (Con minus Oxt) (C) and sex-specific differences (males minus females) in functional connection density in the Oxt-exposed pups (D).

(E) Timeline of the diffusion tensor imaging (DTI) experiment to assess brain structure.

(F) Segmentation showing brain regions of interest (left: mPFC in pink; right: corpus callosum in green and amygdala in violet).

Figure 4. Continued

(G) Representative images showing T2-weighted images, the ADC, and FA of male offspring in Con (above) and Oxt (below) groups. Bar graphs with scatterplots showing lack of differences between unexposed and Oxt-exposed offspring in the ADC and FA of the mPFC (H), amygdala (I) and corpus callosum (J). Significance of FcOISI data determined by 2-tailed Student's t test and FDR-corrected for multiple comparisons on a cluster-wise basis (n = 4–6/treatment/sex). Node degree difference maps were thresholded at a corrected p value of 0.05. DTI data were analyzed with Welch's t-test and expressed as mean $\pm$ SEM (n = 6 per treatment condition; sexes combined because of absence of sex differences).

and the lack of substantial differences in Oxt signaling prompted us to examine the transcriptome of the mPFC, a critical neuroregulatory hub frequently affected in neurodevelopmental disorders,[40,41] with unbiased RNA sequencing. Changes were modest with the largest source of variation being the sex of the offspring and not Oxt exposure (heatmap of differentially expressed genes in Figure 3I). Gene ontology (GO) enrichment analyses and Kyoto Encyclopedia of Genes and Genomes (KEGG) pathway analyses are presented in Figures 3J, 3K, and S4H−S4J (Data S1, S2, and S'3). We confirmed that Oxtr expression was unaltered (Figure S4K). In aggregate, Oxt-induced birth was associated with early communicative delay and impaired empathy-like behaviors especially in males, but these behavioral changes were not accompanied by substantial changes in the mPFC transcriptome.

Birth induction with Oxt sex-specifically alters functional brain connectivity of the offspring

We next asked if perinatal exposure to Oxt could alter functional brain connectivity because of the intricate link between Oxt-Oxtr system and functional connectivity.[42–44] We tested this with *in vivo* optical intrinsic signal imaging (fcOISI) in post-weaning male and female unexposed and Oxt-exposed offspring (P25-30) (Figure 4A). Control rat offspring (Con) exhibited strong positive (reds) ipsilateral correlation adjacent to and contralateral from each seed and strong anticorrelations (blues) between opposed functional networks (e.g., between sensorimotor and retrosplenial cortices). While some of these features were observed in Oxt-exposed rats (Oxt), both ipsilateral and bilateral connections were qualitatively reduced (e.g., in frontal, motor, somatosensory, and visual regions). To quantify these observations, maps of node degree for each group were calculated for all pixels in our field of view by thresholding each pixel's functional connectivity map at z(r) > 0.3 and counting all pixels above this threshold. Control offspring exhibited high connection number (yellows, whites) in retrosplenial, visual and portions of motor regions, while conversely, Oxt-exposed offspring exhibited more global reductions in functional connection number (reds) (Figure 4B). The main group-wise differences (control minus Oxt) occurred within primary and secondary motor, portions of lateral and medial somato-sensory, parietal association, and primary and secondary visual cortices (Figure 4C). Male offspring exhibited higher node degree within lateral parietal and somatosensory regions (Figure 4D, yellows) while females exhibited higher connection number within medial motor, so-matosensory, and retrosplenial cortex (Figure 4D, reds). These changes in functional connectivity were not accompanied by changes in structural connectivity as assessed by *ex vivo* diffusion tensor imaging (DTI) (Figures 4E–4J and S5). Collectively, our data suggested that exposure to Oxt-induced birth causes substantial decreases in functional brain organization of which some changes were sex-specific.

DISCUSSION

In this report, we provide novel preclinical evidence that elective induction of birth with Oxt has neurodevelopmental consequences for the developing offspring. Specifically, we show that Oxt administered for labor crosses the placenta, affects Oxtr expression in the developing brain, and induces a unique pattern of sex-specific abnormalities in neurobehavior and cortical connectivity. Taken together with largely intact measures of maternal-neonatal wellbeing after birth induction with Oxt, our preclinical data indicate that the neurodevelopmental impact is likely directly from Oxt exposure and not indirectly from impaired maternal care. Our work adds significantly to the growing body of animal research suggesting that perinatal exposure to Oxt could be consequential for the offspring.[31,45–48] Our model, however, is distinctive because: (i) Oxt was administered to induce and augment labor making it contextually relevant to modern obstetric practice, (ii) the biological effects of Oxt on cyclical uterine contractility were comprehensively studied and validated previously,[38] (iii) measures of maternal-neonatal wellbeing after Oxt exposure were assayed and confirmed, and (iv) the sophisticated social behavioral repertoire of the offspring from a genetically robust, outbred rat strain was fully leveraged to enable thorough characterization of ASD-specific neurobehavioral changes. By simulating management of human labor with Oxt infusion and ensuring maternal-neonatal wellbeing, results from our work are likely to be translationally relevant than currently existing preclinical models.

Though only 0.1% of maternally administered Oxt was detectable in the neonatal circulation, our results have to be interpreted in the context of notable differences in placental structure and function.[49] Rats have hemotrichorial (3 trophoblast layers) compared to the hemo-monochorial (1 trophoblast layer) placentae in pregnant women,[50,51] raising the possibility that placental Oxt transfer in pregnant women could, in fact, be higher because of reduced interhemal diffusion barrier compared to rodents. This notion of species-specific differences in placental drug transfer is supported by studies on barusiban, an Oxtr antagonist, showing an approximately 5% placental transfer in rabbits (hemodichorial placenta) but a higher 9.1% rate of transfer in primates and humans (hemomonochorial placenta).[52] More notably, during studies with atosiban, an Oxtr antagonist with molecular weight similar to that of Oxt, approximately 12% of the administered atosiban was noted to undergo placental transfer in pregnant women.[53] Our data, therefore, are broadly in alignment with preclinical and human studies demonstrating either direct or indirect evidence for placental Oxt transfer.[14,15,29,31,54,55]

Consistent with the effect of prolonged Oxt exposure on the Oxtr,[32,33,39] we noted a decrease in Oxtr gene and protein expression in the developing brain. Our observations are largely consistent with sex-specific Oxtr downregulation observed at GD18.5 and P9 after perinatal Oxt administration reported by Hsieh et al.,[47] but at odds with those of Hirayama et al.[45] This inconsistency can be partly explained by

differences in the mode of administration (intravenous vs. subcutaneous), the duration of Oxt exposure, and whether or not Oxt administration resulted in birth. Our findings contrast with our previous work with Oxt bolus injection which showed a lack of effect on Oxtr expression in the fetal brain,[56] suggesting that the current results are uniquely driven by sustained exposure to Oxt infusion. In addition, our Oxtr DNA methylation results contrast with that of Kenkel et al.,[31] but could be explained by differences in the experimental paradigm (continuous infusion of Oxt vs. single i.p. injection; sample collection at 8 h vs. 90 min), the Oxtr promoter regions between species (rats vs. prairie voles), and the choice of CpG sites.

Our most important observation was the unique pattern of previously unreported behavioral abnormalities in Oxt-exposed offspring. Early communicative delay in pups after maternal separation could be explained in part by decreased Oxt-ergic signaling secondary to a reduction in Oxtr expression. This is supported by evidence for a reduction in pup USV distress calls after maternal separation in both Oxt and Oxtr knockout (KO) mice.[57,58] Contrary to our hypothesis, however, we did not find evidence for abnormal social behavior, considered *sine qua non* for the diagnosis of ASD. Because behavioral changes appear to be sensitive to Oxtr gene dosage,[59–61] the extent of Oxtr downregulation that we observed was likely below the threshold necessary to cause disruption of social behavior. This notion is compatible with the fact that a majority of children born after Oxt-induced birth show neurotypical development. Therefore, it is likely that an increased dose of Oxt or an underlying genetic vulnerability (gene × Oxt interaction) are potentially more relevant factors in impacting social behavior. Such ideas are supported by our results showing an Oxt dose-dependent decrease in Oxtr expression, evidence for a dose-dependent relationship between Oxt exposure and ASD,[13] and a causal interaction between genetic liability and alteration of Oxt-ergic signaling.[62,63] Though the neurocircuitry mediating empathy-like behaviors need to be probed to better understand the mechanisms, it is well-established that manipulation of Oxt-ergic signaling can influence emotional contagion and OFL. For example, Oxt enhances observational fear, a surrogate for empathy-like behavior, especially in male mice,[21] whereas administration of L-368,899, an Oxt antagonist, can decrease observational fear.[64] Similarly, in prairie voles, KO of the Oxtr resulted in decreased helping behavior when observing distressed conspecifics.[65] Collectively, our behavioral data present a nuanced montage of the neurodevelopmental effects of labor induction with Oxt for the offspring and identify derangement of empathy-like behavior in male offspring as a likely consequence.

Though we did not note decreased Oxtr expression in the mPFC and BLA of P40 animals, regions typically implicated in empathy-like behaviors in rodents, we cannot exclude the possibility of disrupted connectivity between these regions. This is a tangible hypothesis considering that functional connectivity is typically enhanced between the mPFC and the amygdala when observing a distressed conspecific or after intranasal Oxt administration.[66–68] This notion is partly supported by the profound treatment-specific decrease in functional brain connectivity of juvenile offspring after induced birth with Oxt. When analyzed by sex among Oxt-exposed offspring, male and female pups showed unique patterns of regional functional connectivity changes which suggested that the overall impact of Oxt induced birth on functional connectivity in the developing brain is sex-and region-specific. Our results might seem contradictory to the conclusions of a recent prairie vole study that showed an overall increase in functional connectivity, especially in male offspring, after Oxt exposure.[69] These contrasting results can be reconciled because of differences in Oxt administration (intravenous Oxt infusion to induce birth vs. single i.p. administration of Oxt without inducing birth) and the assessment time point (juvenile vs. adult offspring).

Collectively, our proof-of-principle foundational work outlines the wide-ranging impact of elective birth induction with Oxt on neurodevelopmental outcomes and implicates disruption of Oxtr signaling in the developing brain as the most proximate cause. Future work should investigate whether social behavior of the offspring is sensitive to cumulative Oxt dose and underlying genetic vulnerability. With the rising popularity of elective induction, where labor is induced for provider convenience in the absence of maternal or fetal indications,[70,71] our research highlights the critical need for concomitant mechanistic investigations and prospective human studies to evaluate long-term neurodevelopmental health of children after such interventions.

Limitations of the study

Our study has a few limitations that warrant discussion. First, we recognize that results reported here may not be translatable to humans because of significant species differences in the permeability of the placental and the fetal blood-brain barriers that may ultimately affect the extent of Oxt transfer,[50,72,73] and variations in the distribution of the Oxtr in the brain that may modify the potential consequences.[74,75] At best, our results provide evidential support for Oxtr downregulation in the fetal brain after labor induction with Oxt, which until now, has largely been a theoretical concern.[76,77] Second, considerable species differences in neurodevelopmental ontogeny could potentially influence the interpretation of our neurobehavioral outcomes.[74,75,78,79] Though performing these studies in P10 pups, the equivalent of a term human neonate,[78] would seem ideal, it is confounded by the rich social-sensory experiences of the pups during maternal nurturing and littermate contact during the first 10 days of life, in contrast to the absence of these experiences with the *in utero* Oxt exposure paradigm relevant to obstetric practice. Third, because of constraints related to the size of the post-weaning rats, we performed functional connectivity experiments between P25-30. Though these experiments can be correlated with behavioral changes in juvenile offspring, we are unable to extrapolate changes in functional connectivity to DTI features which were measured in adulthood. Similarly, because the amygdala was inaccessible to the fcOISI system, we were unable to directly evaluate functional connectivity between the mPFC and the BLA. Our neurobehavioral results were also limited to the juvenile/adolescent period, so it remains unclear how these developmental neurobehavioral trajectories evolve across the lifespan. Our work does not exclude other causal possibilities that are unrelated to Oxt *per se*, i.e., from interrupting or altering the preordained process of natural labor, such as labor dystocia with oxytocin, the consequence of slightly earlier birth, or the impact of labor induction on fetal signaling to initiate parturition.[80–82] Similarly, there are multiple pathways by which disruption of Oxtr signaling could lead to neurobehavioral impairment through interlinked mechanisms (e.g., perinatal disruption of gamma-aminobutyric acid signaling,

downregulation of the cation chloride transporter KCC2 resulting in excitation-inhibition imbalance, altered synaptogenesis etc.).[29,30,83–85] By adapting our model to transgenic animals, hypotheses related to Oxt signaling deficits could be potentially tested in future experiments. Finally, our animal model provides valuable biological insights into the neurodevelopmental impact of exogenous Oxt exposure at birth, but their applicability to complex human development and behavior is limited and necessitates further clinical research.

STAR★METHODS

Detailed methods are provided in the online version of this paper and include the following:

- KEY RESOURCES TABLE
- RESOURCE AVAILABILITY
  - Lead contact
  - Materials availability
  - Data and code availability
- EXPERIMENTAL MODEL AND STUDY PARTICIPANT DETAILS
- METHOD DETAILS
  - Pup retrieval test
  - Qualitative assessment of maternal nurturing behavior
  - Licking and grooming 'pen mark' assay
  - Weigh-suckle-weigh (WSW) method to assess milk intake
  - Quantification of Oxt in the fetal plasma and brain
  - Stable isotope labeled Oxt (SIL-Oxt) for assessment of placental transfer
  - Evaluation of OxtR gene and protein expression in the brain
  - DNA methylation analysis of the OxtR promoter region
  - Oxt plasma assays at P40
  - Assessment of behavioral phenotype after Oxt-induced birth
  - Maternal isolation-induced ultrasonic vocalizations
  - Elevated plus maze
  - Juvenile social play
  - Spontaneous alternation Y-maze
  - Juvenile dyad USVs
  - Acoustic startle/prepulse inhibition
  - Social approach
  - Observational fear learning
  - Assessment of puberty onset
  - RNA-seq to assess the impact of Oxt on the medial prefrontal cortex transcriptome
  - Functional connectivity mapping with optical intrinsic signal imaging
  - *Ex vivo* DTI for structural connectivity assessment
- QUANTIFICATION AND STATISTICAL ANALYSIS

SUPPLEMENTAL INFORMATION

Supplemental information can be found online at https://doi.org/10.1016/j.isci.2024.108960.

AUTHOR CONTRIBUTIONS

A.P. conceived the study design, planned the experiments, and wrote the manuscript with help from all co-authors. A.P. and T.G. conducted the animal surgery, and performed the molecular biology experiments. S.G. performed the video analysis for maternal behaviors and generated the data for the manuscript. E.T. performed the statistical analysis and generated the figures and tables for RNA-seq data. Y.A.G., J.H.S.,

REFERENCES

1. Zhang, J., Branch, D.W., Ramirez, M.M., Laughon, S.K., Reddy, U., Hoffman, M., Bailit, J., Kominiarek, M., Chen, Z., and Hibbard, J.U. (2011). Oxytocin regimen for labor augmentation, labor progression, and perinatal outcomes. Obstet. Gynecol. *118*, 249–256. https://doi.org/10.1097/AOG.0b013e3182220192.

2. Kernberg, A., and Caughey, A.B. (2017). Augmentation of Labor: A Review of Oxytocin Augmentation and Active Management of Labor. Obstet. Gynecol. Clin. North Am. *44*, 593–600. https://doi.org/10.1016/j.ogc.2017.08.012.

3. Gregory, S.G., Anthopolos, R., Osgood, C.E., Grotegut, C.A., and Miranda, M.L. (2013). Association of autism with induced or augmented childbirth in North Carolina Birth Record (1990-1998) and Education Research (1997-2007) databases. JAMA Pediatr. *167*, 959–966. https://doi.org/10.1001/jamapediatrics.2013.2904.

4. Weisman, O., Agerbo, E., Carter, C.S., Harris, J.C., Uldbjerg, N., Henriksen, T.B., Thygesen, M., Mortensen, P.B., Leckman, J.F., and Dalsgaard, S. (2015). Oxytocin-augmented labor and risk for autism in males. Behav. Brain Res. *284*, 207–212. https://doi.org/10.1016/j.bbr.2015.02.028.

5. Friedlander, E., Feldstein, O., Mankuta, D., Yaari, M., Harel-Gadassi, A., Ebstein, R.P., and Yirmiya, N. (2017). Social impairments among children perinatally exposed to oxytocin or oxytocin receptor antagonist. Early Hum. Dev. *106–107*, 13–18. https://doi.org/10.1016/j.earlhumdev.2017.01.008.

6. Smallwood, M., Sareen, A., Baker, E., Hannusch, R., Kwessi, E., and Williams, T. (2016). Increased Risk of Autism Development in Children Whose Mothers Experienced Birth Complications or Received Labor and Delivery Drugs. ASN Neuro *8*, 1759091416659742. https://doi.org/10.1177/1759091416659742.

7. Burger, R.J., Mol, B.W., Ganzevoort, W., Gordijn, S.J., Pajkrt, E., Van Der Post, J.A.M., De Groot, C.J.M., and Ravelli, A.C.J. (2023). Offspring school performance at age 12 after induction of labor vs non-intervention at term: A linked cohort study. Acta Obstet. Gynecol. Scand. *102*, 486–495. https://doi.org/10.1111/aogs.14520.

8. Freedman, D., Brown, A.S., Shen, L., and Schaefer, C.A. (2015). Perinatal oxytocin increases the risk of offspring bipolar disorder and childhood cognitive impairment. J. Affect. Disord. *173*, 65–72. https://doi.org/10.1016/j.jad.2014.10.052.

9. Kurth, L., and Haussmann, R. (2011). Perinatal Pitocin as an early ADHD biomarker: neurodevelopmental risk? J. Atten. Disord. *15*, 423–431. https://doi.org/10.1177/1087054710397800.

10. Oberg, A.S., D'Onofrio, B.M., Rickert, M.E., Hernandez-Diaz, S., Ecker, J.L., Almqvist, C., Larsson, H., Lichtenstein, P., and Bateman, B.T. (2016). Association of Labor Induction With Offspring Risk of Autism Spectrum Disorders. JAMA Pediatr. *170*, e160965. https://doi.org/10.1001/jamapediatrics.2016.0965.

11. Wiggs, K.K., Rickert, M.E., Hernandez-Diaz, S., Bateman, B.T., Almqvist, C., Larsson, H., Lichtenstein, P., Oberg, A.S., and D'Onofrio, B.M. (2017). A Family-Based Study of the Association Between Labor Induction and Offspring Attention-Deficit Hyperactivity Disorder and Low Academic Achievement. Behav. Genet. *47*, 383–393. https://doi.org/10.1007/s10519-017-9852-4.

12. Guastella, A.J., Cooper, M.N., White, C.R.H., White, M.K., Pennell, C.E., and Whitehouse, A.J.O. (2018). Does perinatal exposure to exogenous oxytocin influence child behavioural problems and autistic-like behaviours to 20 years of age? J. Child Psychol. Psychiatry *59*, 1323–1332. https://doi.org/10.1111/jcpp.12924.

13. Soltys, S.M., Scherbel, J.R., Kurian, J.R., Diebold, T., Wilson, T., Hedden, L., Groesch, K., Diaz-Sylvester, P.L., Botchway, A., Campbell, P., and Loret de Mola, J.R. (2020). An association of intrapartum synthetic oxytocin dosing and the odds of developing autism. Autism *24*, 1400–1410. https://doi.org/10.1177/1362361320902903.

14. Malek, A., Blann, E., and Mattison, D.R. (1996). Human placental transport of oxytocin. J. Matern. Fetal Med. *5*, 245–255. https://doi.org/10.1002/(SICI)1520-6661(199609/10)5:5<245::AID-MFM3>3.0.CO;2-H.

15. Nathan, N.O., Hedegaard, M., Karlsson, G., Knudsen, L.E., and Mathiesen, L. (2021). Intrapartum transfer of oxytocin across the human placenta: An ex vivo perfusion experiment. Placenta *112*, 105–110. https://doi.org/10.1016/j.placenta.2021.07.289.

16. Kramer, E.E. (1957). The intravenous pitocin drip in obstetrics. Surg. Clin. North Am. *37*, 435–446. https://doi.org/10.1016/s0039-6109(16)35137-4.

17. Ryan, T.J. (1958). On the safety of the pitocin drip. J. Obstet. Gynaecol. Br. Emp. *65*, 71–77. https://doi.org/10.1111/j.1471-0528.1958.tb06211.x.

18. Williams, P.C., and McMahon, T.B. (1956). Intravenous pitocin infusion in obstetrics; a report of 210 consecutive cases. Am. J. Obstet. Gynecol. *71*, 1264–1273. https://doi.org/10.1016/0002-9378(56)90435-5.

19. Lee, H.J., Macbeth, A.H., Pagani, J.H., and Young, W.S., 3rd (2009). Oxytocin: the great facilitator of life. Prog. Neurobiol. *88*, 127–151. https://doi.org/10.1016/j.pneurobio.2009.04.001.

20. Burkett, J.P., Andari, E., Johnson, Z.V., Curry, D.C., de Waal, F.B.M., and Young, L.J. (2016). Oxytocin-dependent consolation behavior in rodents. Science *351*, 375–378. https://doi.org/10.1126/science.aac4785.

21. Pisansky, M.T., Hanson, L.R., Gottesman, I.I., and Gewirtz, J.C. (2017). Oxytocin enhances observational fear in mice. Nat. Commun. *8*, 2102. https://doi.org/10.1038/s41467-017-02279-5.

22. Carter, C.S., Kenkel, W.M., MacLean, E.L., Wilson, S.R., Perkeybile, A.M., Yee, J.R., Ferris, C.F., Nazarloo, H.P., Porges, S.W., Davis, J.M., et al. (2020). Is Oxytocin "Nature's Medicine"? Pharmacol. Rev. *72*, 829–861. https://doi.org/10.1124/pr.120.019398.

23. Baumgartner, T., Heinrichs, M., Vonlanthen, A., Fischbacher, U., and Fehr, E. (2008). Oxytocin shapes the neural circuitry of trust and trust adaptation in humans. Neuron *58*, 639–650. https://doi.org/10.1016/j.neuron.2008.04.009.

24. Carter, C.S. (2014). Oxytocin pathways and the evolution of human behavior. Annu. Rev. Psychol. *65*, 17–39. https://doi.org/10.1146/annurev-psych-010213-115110.

25. Kosfeld, M., Heinrichs, M., Zak, P.J., Fischbacher, U., and Fehr, E. (2005). Oxytocin increases trust in humans. Nature *435*, 673–676. https://doi.org/10.1038/nature03701.

26. Rodrigues, S.M., Saslow, L.R., Garcia, N., John, O.P., and Keltner, D. (2009). Oxytocin receptor genetic variation relates to empathy and stress reactivity in humans. Proc. Natl. Acad. Sci. USA *106*, 21437–21441. https://doi.org/10.1073/pnas.0909579106.

27. Monks, D.T., and Palanisamy, A. (2019). Intrapartum oxytocin: time to focus on longer term consequences? Anaesthesia 74, 1219–1222. https://doi.org/10.1111/anae.14746.

28. Monks, D.T., and Palanisamy, A. (2021). Oxytocin: at birth and beyond. A systematic review of the long-term effects of peripartum oxytocin. Anaesthesia 76, 1526–1537. https://doi.org/10.1111/anae.15553.

29. Tyzio, R., Cossart, R., Khalilov, I., Minlebaev, M., Hübner, C.A., Represa, A., Ben-Ari, Y., and Khazipov, R. (2006). Maternal oxytocin triggers a transient inhibitory switch in GABA signaling in the fetal brain during delivery. Science 314, 1788–1792. https://doi.org/10.1126/science.1133212.

30. Tyzio, R., Nardou, R., Ferrari, D.C., Tsintsadze, T., Shahrokhi, A., Eftekhari, S., Khalilov, I., Tsintsadze, V., Brouchoud, C., Chazal, G., et al. (2014). Oxytocin-mediated GABA inhibition during delivery attenuates autism pathogenesis in rodent offspring. Science 343, 675–679. https://doi.org/10.1126/science.1247190.

31. Kenkel, W.M., Perkeybile, A.M., Yee, J.R., Pournajafi-Nazarloo, H., Lillard, T.S., Ferguson, E.F., Wroblewski, K.L., Ferris, C.F., Carter, C.S., and Connelly, J.J. (2019). Behavioral and epigenetic consequences of oxytocin treatment at birth. Sci. Adv. 5, eaav2244. https://doi.org/10.1126/sciadv.aav2244.

32. Phaneuf, S., Rodríguez Liñares, B., TambyRaja, R.L., MacKenzie, I.Z., and López Bernal, A. (2000). Loss of myometrial oxytocin receptors during oxytocin-induced and oxytocin-augmented labour. J. Reprod. Fertil. 120, 91–97.

33. Robinson, C., Schumann, R., Zhang, P., and Young, R.C. (2003). Oxytocin-induced desensitization of the oxytocin receptor. Am. J. Obstet. Gynecol. 188, 497–502.

34. O' Sullivan, C., Wilson, E., and Beckmann, M. (2022). Five-year trends in induction of labour in a large Australian metropolitan maternity service. Aust. N. Z. J. Obstet. Gynaecol. 62, 407–412. https://doi.org/10.1111/ajo.13486.

35. Clark, S.L., Miller, D.D., Belfort, M.A., Dildy, G.A., Frye, D.K., and Meyers, J.A. (2009). Neonatal and maternal outcomes associated with elective term delivery. Am. J. Obstet. Gynecol. 200, 156.e1-4. https://doi.org/10.1016/j.ajog.2008.08.068.

36. Dögl, M., Romundstad, P., Berntzen, L.D., Fremgaarden, O.C., Kirial, K., Kjøllesdal, A.M., Nygaard, B.S., Robberstad, L., Steen, T., Tappert, C., et al. (2018). Elective induction of labor: A prospective observational study. PLoS One 13, e0208098. https://doi.org/10.1371/journal.pone.0208098.

37. Swift, E.M., Gunnarsdottir, J., Zoega, H., Bjarnadottir, R.I., Steingrimsdottir, T., and Einarsdottir, K. (2022). Trends in labor induction indications: A 20-year population-based study. Acta Obstet. Gynecol. Scand. 101, 1422–1430. https://doi.org/10.1111/aogs.14447.

38. Giri, T., Jiang, J., Xu, Z., McCarthy, R., Halabi, C.M., Tycksen, E., Cahill, A.G., England, S.K., and Palanisamy, A. (2022). Labor induction with oxytocin in pregnant rats is not associated with oxidative stress in the fetal brain. Sci. Rep. 12, 3143. https://doi.org/10.1038/s41598-022-07236-x.

39. Balki, M., Erik-Soussi, M., Kingdom, J., and Carvalho, J.C.A. (2013). Oxytocin pretreatment attenuates oxytocin-induced contractions in human myometrium in vitro. Anesthesiology 119, 552–561. https://doi.org/10.1097/ALN.0b013e318297d347.

40. Schubert, D., Martens, G.J.M., and Kolk, S.M. (2015). Molecular underpinnings of prefrontal cortex development in rodents provide insights into the etiology of neurodevelopmental disorders. Mol. Psychiatry 20, 795–809. https://doi.org/10.1038/mp.2014.147.

41. Chini, M., and Hanganu-Opatz, I.L. (2021). Prefrontal Cortex Development in Health and Disease: Lessons from Rodents and Humans. Trends Neurosci. 44, 227–240. https://doi.org/10.1016/j.tins.2020.10.017.

42. Hernandez, L.M., Krasileva, K., Green, S.A., Sherman, L.E., Ponting, C., McCarron, R., Lowe, J.K., Geschwind, D.H., Bookheimer, S.Y., and Dapretto, M. (2017). Additive effects of oxytocin receptor gene polymorphisms on reward circuitry in youth with autism. Mol. Psychiatry 22, 1134–1139. https://doi.org/10.1038/mp.2016.209.

43. Hernandez, L.M., Lawrence, K.E., Padgaonkar, N.T., Inada, M., Hoekstra, J.N., Lowe, J.K., Eilbott, J., Jack, A., Aylward, E., Gaab, N., et al. (2020). Imaging-genetics of sex differences in ASD: distinct effects of OXTR variants on brain connectivity. Transl. Psychiatry 10, 82. https://doi.org/10.1038/s41398-020-0750-9.

44. Riem, M.M.E., van IJzendoorn, M.H., Tops, M., Boksem, M.A.S., Rombouts, S.A.R.B., and Bakermans-Kranenburg, M.J. (2012). No laughing matter: intranasal oxytocin administration changes functional brain connectivity during exposure to infant laughter. Neuropsychopharmacology 37, 1257–1266. https://doi.org/10.1038/npp.2011.313.

45. Hirayama, T., Hiraoka, Y., Kitamura, E., Miyazaki, S., Horie, K., Fukuda, T., Hidema, S., Koike, M., Itakura, A., Takeda, S., and Nishimori, K. (2020). Oxytocin induced labor causes region and sex-specific transient oligodendrocyte cell death in neonatal mouse brain. J. Obstet. Gynaecol. Res. 46, 66–78. https://doi.org/10.1111/jog.14149.

46. Kitamura, E., Koike, M., Hirayama, T., Sunabori, T., Kameda, H., Hioki, H., Takeda, S., and Itakura, A. (2021). Susceptibility of subregions of prefrontal cortex and corpus callosum to damage by high-dose oxytocin-induced labor in male neonatal mice. PLoS One 16, e0256693. https://doi.org/10.1371/journal.pone.0256693.

47. Hsieh, F.F., Korsunsky, I., Shih, A.J., Moss, M.A., Chatterjee, P.K., Deshpande, J., Xue, X., Madankumar, S., Kumar, G., Rochelson, B., and Metz, C.N. (2022). Maternal oxytocin administration modulates gene expression in the brains of perinatal mice. J. Perinat. Med. 50, 207–218. https://doi.org/10.1515/jpm-2020-0525.

48. Boksa, P., Zhang, Y., and Nouel, D. (2015). Maternal Oxytocin Administration Before Birth Influences the Effects of Birth Anoxia on the Neonatal Rat Brain. Neurochem. Res. 40, 1631–1643. https://doi.org/10.1007/s11064-015-1645-7.

49. Schmidt, A., Schmidt, A., and Markert, U.R. (2021). The road (not) taken - Placental transfer and interspecies differences. Placenta 115, 70–77. https://doi.org/10.1016/j.placenta.2021.09.011.

50. Furukawa, S., Kuroda, Y., and Sugiyama, A. (2014). A comparison of the histological structure of the placenta in experimental animals. J. Toxicol. Pathol. 27, 11–18. https://doi.org/10.1293/tox.2013-0060.

51. Furukawa, S., Tsuji, N., and Sugiyama, A. (2019). Morphology and physiology of rat placenta for toxicological evaluation. J. Toxicol. Pathol. 32, 1–17. https://doi.org/10.1293/tox.2018-0042.

52. Helmer, H., Saleh, L., Petricevic, L., Knöfler, M., and Reinheimer, T.M. (2020). Barusiban, a selective oxytocin receptor antagonist: placental transfer in rabbit, monkey, and humandagger. Biol. Reprod. 103, 135–143. https://doi.org/10.1093/biolre/ioaa048.

53. Valenzuela, G.J., Craig, J., Bernhardt, M.D., and Holland, M.L. (1995). Placental passage of the oxytocin antagonist atosiban. Am. J. Obstet. Gynecol. 172, 1304–1306. https://doi.org/10.1016/0002-9378(95)91497-8.

54. Dawood, M.Y., Khan-Dawood, F.S., Ayromlooi, J., and Tobias, M. (1983). Maternal and fetal plasma oxytocin levels during pregnancy and parturition in the sheep. Am. J. Obstet. Gynecol. 147, 584–588.

55. Dawood, M.Y., Lauersen, N.H., Trivedi, D., Ylikorkala, O., and Fuchs, F. (1979). Studies of oxytocin in the baboon during pregnancy and delivery. Acta Endocrinol. 91, 704–718.

56. Palanisamy, A., Giri, T., Jiang, J., Bice, A., Quirk, J.D., Conyers, S.B., Maloney, S.E., Raghuraman, N., Bauer, A.Q., Garbow, J.R., and Wozniak, D.F. (2020). In utero exposure to transient ischemia-hypoxemia promotes long-term neurodevelopmental abnormalities in male rat offspring. JCI Insight 5, e133172. https://doi.org/10.1172/jci.insight.133172.

57. Winslow, J.T., Hearn, E.F., Ferguson, J., Young, L.J., Matzuk, M.M., and Insel, T.R. (2000). Infant vocalization, adult aggression, and fear behavior of an oxytocin null mutant mouse. Horm. Behav. 37, 145–155. https://doi.org/10.1006/hbeh.1999.1566.

58. Takayanagi, Y., Yoshida, M., Bielsky, I.F., Ross, H.E., Kawamata, M., Onaka, T., Yanagisawa, T., Kimura, T., Matzuk, M.M., Young, L.J., and Nishimori, K. (2005). Pervasive social deficits, but normal parturition, in oxytocin receptor-deficient mice. Proc. Natl. Acad. Sci. USA 102, 16096–16101. https://doi.org/10.1073/pnas.0505312102.

59. Pobbe, R.L.H., Pearson, B.L., Defensor, E.B., Bolivar, V.J., Young, W.S., 3rd, Lee, H.J., Blanchard, D.C., and Blanchard, R.J. (2012). Oxytocin receptor knockout mice display deficits in the expression of autism-related behaviors. Horm. Behav. 61, 436–444. https://doi.org/10.1016/j.yhbeh.2011.10.010.

60. Sala, M., Braida, D., Donzelli, A., Martucci, R., Busnelli, M., Bulgheroni, E., Rubino, T., Parolaro, D., Nishimori, K., and Chini, B. (2013). Mice heterozygous for the oxytocin receptor gene (Oxtr(+/-)) show impaired social behaviour but not increased aggression or cognitive inflexibility: evidence of a selective haploinsufficiency gene effect. J. Neuroendocrinol. 25, 107–118. https://doi.org/10.1111/j.1365-2826.2012.02385.x.

61. Sala, M., Braida, D., Lentini, D., Busnelli, M., Bulgheroni, E., Capurro, V., Finardi, A., Donzelli, A., Pattini, L., Rubino, T., et al. (2011). Pharmacologic rescue of impaired cognitive flexibility, social deficits, increased aggression, and seizure susceptibility in oxytocin receptor null mice: a neurobehavioral model of autism. Biol.

Psychiatry *69*, 875–882. https://doi.org/10.1016/j.biopsych.2010.12.022.

62. García-Alcón, A., González-Peñas, J., Weckx, E., Penzol, M.J., Gurriarán, X., Costas, J., Díaz-Caneja, C.M., Moreno, C., Hernández, P., Arango, C., and Parellada, M. (2023). Oxytocin Exposure in Labor and its Relationship with Cognitive Impairment and the Genetic Architecture of Autism. J. Autism Dev. Disord. *53*, 66–79. https://doi.org/10.1007/s10803-021-05409-7.

63. Friedlander, E., Yirmiya, N., Laiba, E., Harel-Gadassi, A., Yaari, M., Feldstein, O., Mankuta, D., and Israel, S. (2019). Cumulative Risk of the Oxytocin Receptor Gene Interacts with Prenatal Exposure to Oxytocin Receptor Antagonist to Predict Children's Social Communication Development. Autism Res. *12*, 1087–1100. https://doi.org/10.1002/aur.2111.

64. Sakaguchi, T., Iwasaki, S., Okada, M., Okamoto, K., and Ikegaya, Y. (2018). Ethanol facilitates socially evoked memory recall in mice by recruiting pain-sensitive anterior cingulate cortical neurons. Nat. Commun. *9*, 3526. https://doi.org/10.1038/s41467-018-05894-y.

65. Kitano, K., Yamagishi, A., Horie, K., Nishimori, K., and Sato, N. (2022). Helping behavior in prairie voles: A model of empathy and the importance of oxytocin. iScience *25*, 103991. https://doi.org/10.1016/j.isci.2022.103991.

66. Ito, M., Erisir, A., and Morozov, A. (2015). Observation of Distressed Conspecific as a Model of Emotional Trauma Generates Silent Synapses in the Prefrontal-Amygdala Pathway and Enhances Fear Learning, but Ketamine Abolishes those Effects. Neuropsychopharmacology *40*, 2536–2545. https://doi.org/10.1038/npp.2015.100.

67. Dodhia, S., Hosanagar, A., Fitzgerald, D.A., Labuschagne, I., Wood, A.G., Nathan, P.J., and Phan, K.L. (2014). Modulation of resting-state amygdala-frontal functional connectivity by oxytocin in generalized social anxiety disorder. Neuropsychopharmacology *39*, 2061–2069. https://doi.org/10.1038/npp.2014.53.

68. Sripada, C.S., Phan, K.L., Labuschagne, I., Welsh, R., Nathan, P.J., and Wood, A.G. (2013). Oxytocin enhances resting-state connectivity between amygdala and medial frontal cortex. Int. J. Neuropsychopharmacol. *16*, 255–260. https://doi.org/10.1017/S1461145712000533.

69. Kenkel, W.M., Ortiz, R.J., Yee, J.R., Perkeybile, A.M., Kulkarni, P., Carter, C.S., Cushing, B.S., and Ferris, C.F. (2023). Neuroanatomical and functional consequences of oxytocin treatment at birth in prairie voles. Psychoneuroendocrinology *150*, 106025. https://doi.org/10.1016/j.psyneuen.2023.106025.

70. Grobman, W.A., Rice, M.M., Reddy, U.M., Tita, A.T.N., Silver, R.M., Mallett, G., Hill, K., Thom, E.A., El-Sayed, Y.Y., Perez-Delboy, A., et al. (2018). Labor Induction versus Expectant Management in Low-Risk Nulliparous Women. N. Engl. J. Med. *379*, 513–523. https://doi.org/10.1056/NEJMoa1800566.

71. Souter, V., Painter, I., Sitcov, K., and Caughey, A.B. (2019). Maternal and newborn outcomes with elective induction of labor at term. Am. J. Obstet. Gynecol. *220*, 273.e1–273.e11. https://doi.org/10.1016/j.ajog.2019.01.223.

72. Schmidt, A., Morales-Prieto, D.M., Pastuschek, J., Fröhlich, K., and Markert, U.R. (2015). Only humans have human placentas: molecular differences between mice and humans. J. Reprod. Immunol. *108*, 65–71. https://doi.org/10.1016/j.jri.2015.03.001.

73. Aday, S., Cecchelli, R., Hallier-Vanuxeem, D., Dehouck, M.P., and Ferreira, L. (2016). Stem Cell-Based Human Blood-Brain Barrier Models for Drug Discovery and Delivery. Trends Biotechnol. *34*, 382–393. https://doi.org/10.1016/j.tibtech.2016.01.001.

74. Freeman, S.M., and Young, L.J. (2016). Comparative Perspectives on Oxytocin and Vasopressin Receptor Research in Rodents and Primates: Translational Implications. J. Neuroendocrinol. *28*. https://doi.org/10.1111/jne.12382.

75. Vaidyanathan, R., and Hammock, E.A.D. (2017). Oxytocin receptor dynamics in the brain across development and species. Dev. Neurobiol. *77*, 143–157. https://doi.org/10.1002/dneu.22403.

76. Wahl, R.U.R. (2004). Could oxytocin administration during labor contribute to autism and related behavioral disorders?–A look at the literature. Med. Hypotheses *63*, 456–460. https://doi.org/10.1016/j.mehy.2004.03.008.

77. Gottlieb, M.M. (2019). A Mathematical Model Relating Pitocin Use during Labor with Offspring Autism Development in terms of Oxytocin Receptor Desensitization in the Fetal Brain. Comput. Math. Methods Med. *2019*, 8276715. https://doi.org/10.1155/2019/8276715.

78. Clancy, B., Darlington, R.B., and Finlay, B.L. (2001). Translating developmental time across mammalian species. Neuroscience *105*, 7–17.

79. Clancy, B., Kersh, B., Hyde, J., Darlington, R.B., Anand, K.J.S., and Finlay, B.L. (2007). Web-based method for translating neurodevelopment from laboratory species to humans. Neuroinformatics *5*, 79–94.

80. Dawood, M.Y., Wang, C.F., Gupta, R., and Fuchs, F. (1978). Fetal contribution to oxytocin in human labor. Obstet. Gynecol. *52*, 205–209.

81. Gao, L., Rabbitt, E.H., Condon, J.C., Renthal, N.E., Johnston, J.M., Mitsche, M.A., Chambon, P., Xu, J., O'Malley, B.W., and Mendelson, C.R. (2015). Steroid receptor coactivators 1 and 2 mediate fetal-to-maternal signaling that initiates parturition. J. Clin. Invest. *125*, 2808–2824. https://doi.org/10.1172/JCI78544.

82. Yoshihara, M., Mizutani, S., Matsumoto, K., Kato, Y., Masuo, Y., Harumasa, A., Iyoshi, S., Tano, S., Mizutani, H., Kotani, T., et al. (2023). The balance between fetal oxytocin and placental leucine aminopeptidase (P-LAP) controls human uterine contraction around labor onset. Eur. J. Obstet. Gynecol. Reprod. Biol. X *19*, 100210. https://doi.org/10.1016/j.eurox.2023.100210.

83. Khazipov, R., Tyzio, R., and Ben-Ari, Y. (2008). Effects of oxytocin on GABA signalling in the foetal brain during delivery. Prog. Brain Res. *170*, 243–257. https://doi.org/10.1016/S0079-6123(08)00421-4.

84. Leonzino, M., Busnelli, M., Antonucci, F., Verderio, C., Mazzanti, M., and Chini, B. (2016). The Timing of the Excitatory-to-Inhibitory GABA Switch Is Regulated by the Oxytocin Receptor via KCC2. Cell Rep. *15*, 96–103. https://doi.org/10.1016/j.celrep.2016.03.013.

85. Ripamonti, S., Ambrozkiewicz, M.C., Guzzi, F., Gravati, M., Biella, G., Bormuth, I., Hammer, M., Tuffy, L.P., Sigler, A., Kawabe, H., et al. (2017). Transient oxytocin signaling primes the development and function of excitatory hippocampal neurons. Elife *6*, e22466. https://doi.org/10.7554/eLife.22466.

86. Robinson, M.D., McCarthy, D.J., and Smyth, G.K. (2010). edgeR: a Bioconductor package for differential expression analysis of digital gene expression data. Bioinformatics *26*, 139–140. https://doi.org/10.1093/bioinformatics/btp616.

87. Ritchie, M.E., Phipson, B., Wu, D., Hu, Y., Law, C.W., Shi, W., and Smyth, G.K. (2015). limma powers differential expression analyses for RNA-sequencing and microarray studies. Nucleic Acids Res. *43*, e47. https://doi.org/10.1093/nar/gkv007.

88. Liu, R., Holik, A.Z., Su, S., Jansz, N., Chen, K., Leong, H.S., Blewitt, M.E., Asselin-Labat, M.L., Smyth, G.K., and Ritchie, M.E. (2015). Why weight? Modelling sample and observational level variability improves power in RNA-seq analyses. Nucleic Acids Res. *43*, e97. https://doi.org/10.1093/nar/gkv412.

89. Luo, W., Friedman, M.S., Shedden, K., Hankenson, K.D., and Woolf, P.J. (2009). GAGE: generally applicable gene set enrichment for pathway analysis. BMC Bioinf. *10*, 161. https://doi.org/10.1186/1471-2105-10-161.

90. Zhao, S., Guo, Y., Sheng, Q., and Shyr, Y. (2014). Advanced heat map and clustering analysis using heatmap3. BioMed Res. Int. *2014*, 986048. https://doi.org/10.1155/2014/986048.

91. Luo, W., and Brouwer, C. (2013). Pathview: an R/Bioconductor package for pathway-based data integration and visualization. Bioinformatics *29*, 1830–1831. https://doi.org/10.1093/bioinformatics/btt285.

92. Langfelder, P., and Horvath, S. (2008). WGCNA: an R package for weighted correlation network analysis. BMC Bioinf. *9*, 559. https://doi.org/10.1186/1471-2105-9-559.

93. Yu, G., Wang, L.G., Han, Y., and He, Q.Y. (2012). clusterProfiler: an R package for comparing biological themes among gene clusters. OMICS *16*, 284–287. https://doi.org/10.1089/omi.2011.0118.

94. Hakon, J., Quattromani, M.J., Sjölund, C., Tomasevic, G., Carey, L., Lee, J.M., Ruscher, K., Wieloch, T., and Bauer, A.Q. (2018). Multisensory stimulation improves functional recovery and resting-state functional connectivity in the mouse brain after stroke. Neuroimage. Clin. *17*, 717–730. https://doi.org/10.1016/j.nicl.2017.11.022.

95. Lee, Y.M., Mu, A., Wallace, M., Gengatharan, J.M., Furst, A., Bode, L., Metallo, C.M., and Ayres, J.S. (2021). Microbiota control of maternal behavior regulates early postnatal growth of offspring. Sci. Adv. *7*, eabe6563. https://doi.org/10.1126/sciadv.abe6563.

96. Jiang, J., Giri, T., Raghuraman, N., Cahill, A.G., and Palanisamy, A. (2021). Impact of intrauterine fetal resuscitation with oxygen on oxidative stress in the developing rat brain. Sci. Rep. *11*, 9798. https://doi.org/10.1038/s41598-021-89299-w.

97. Beery, A.K., McEwen, L.M., MacIsaac, J.L., Francis, D.D., and Kobor, M.S. (2016). Natural variation in maternal care and cross-tissue patterns of oxytocin receptor gene

methylation in rats. Horm. Behav. *77*, 42–52. https://doi.org/10.1016/j.yhbeh.2015.05.022.

98. Hofer, M.A. (1996). Multiple regulators of ultrasonic vocalization in the infant rat. Psychoneuroendocrinology *21*, 203–217. https://doi.org/10.1016/0306-4530(95)00042-9.

99. Hofer, M.A., Brunelli, S.A., and Shair, H.N. (1994). Potentiation of isolation-induced vocalization by brief exposure of rat pups to maternal cues. Dev. Psychobiol. *27*, 503–517. https://doi.org/10.1002/dev.420270804.

100. Chen, J., Lambo, M.E., Ge, X., Dearborn, J.T., Liu, Y., McCullough, K.B., Swift, R.G., Tabachnick, D.R., Tian, L., Noguchi, K., et al. (2021). A MYT1L syndrome mouse model recapitulates patient phenotypes and reveals altered brain development due to disrupted neuronal maturation. Neuron *109*, 3775–3792.e14. https://doi.org/10.1016/j.neuron.2021.09.009.

101. Fereshetyan, K., Chavushyan, V., Danielyan, M., and Yenkoyan, K. (2021). Assessment of behavioral, morphological and electrophysiological changes in prenatal and postnatal valproate induced rat models of autism spectrum disorder. Sci. Rep. *11*, 23471. https://doi.org/10.1038/s41598-021-02994-6.

102. Izumi, Y., Kitabayashi, R., Funatsu, M., Izumi, M., Yuede, C., Hartman, R.E., Wozniak, D.F., and Zorumski, C.F. (2005). A single day of ethanol exposure during development has persistent effects on bi-directional plasticity, N-methyl-D-aspartate receptor function and ethanol sensitivity. Neuroscience *136*, 269–279. https://doi.org/10.1016/j.neuroscience.2005.07.015.

103. Wozniak, D.F., Diggs-Andrews, K.A., Conyers, S., Yuede, C.M., Dearborn, J.T., Brown, J.A., Tokuda, K., Izumi, Y., Zorumski, C.F., and Gutmann, D.H. (2013). Motivational disturbances and effects of L-dopa administration in neurofibromatosis-1 model mice. PLoS One *8*, e66024. https://doi.org/10.1371/journal.pone.0066024.

104. Smith, J.T., and Waddell, B.J. (2000). Increased fetal glucocorticoid exposure delays puberty onset in postnatal life. Endocrinology *141*, 2422–2428. https://doi.org/10.1210/endo.141.7.7541.

105. Ajayi, A.F., and Akhigbe, R.E. (2020). Staging of the estrous cycle and induction of estrus in experimental rodents: an update. Fertil. Res. Pract. *6*, 5. https://doi.org/10.1186/s40738-020-00074-3.

106. Bauer, A.Q., Kraft, A.W., Wright, P.W., Snyder, A.Z., Lee, J.M., and Culver, J.P. (2014). Optical imaging of disrupted functional connectivity following ischemic stroke in mice. Neuroimage *99*, 388–401. https://doi.org/10.1016/j.neuroimage.2014.05.051.

107. Mitra, A., Kraft, A., Wright, P., Acland, B., Snyder, A.Z., Rosenthal, Z., Czerniewski, L., Bauer, A., Snyder, L., Culver, J., et al. (2018). Spontaneous Infra-slow Brain Activity Has Unique Spatiotemporal Dynamics and Laminar Structure. Neuron *98*, 297–305.e6. https://doi.org/10.1016/j.neuron.2018.03.015.

108. Avants, B.B., Tustison, N.J., Stauffer, M., Song, G., Wu, B., and Gee, J.C. (2014). The Insight ToolKit image registration framework. Front. Neuroinform. *8*, 44. https://doi.org/10.3389/fninf.2014.00044.

109. Horsfield, M.A., and Jones, D.K. (2002). Applications of diffusion-weighted and diffusion tensor MRI to white matter diseases - a review. NMR Biomed. *15*, 570–577. https://doi.org/10.1002/nbm.787.

110. Mori, S., and Zhang, J. (2006). Principles of diffusion tensor imaging and its applications to basic neuroscience research. Neuron *51*, 527–539. https://doi.org/10.1016/j.neuron.2006.08.012.

111. Quirk, J.D., Bretthorst, G.L., Garbow, J.R., and Ackerman, J.J.H. (2019). Magnetic resonance data modeling: The Bayesian analysis toolbox. Concepts Magn. Reson. *47A*, 1–13.

STAR★METHODS

KEY RESOURCES TABLE

REAGENT or RESOURCE	SOURCE	IDENTIFIER
Antibodies		
Rabbit polyclonal anti-OxtR antibody	www.origene.com	TA351476
Rabbit polyclonal anti-cyclophilin antibody	www.cellsignal.com	Cat# 2175; RRID: AB_2169116
Anti-rabbit IgG, HRP-linked antibody	www.cellsignal.com	Cat# 7074; RRID: AB_2099233
Chemicals, peptides, and recombinant proteins		
Oxytocin (Syntocinon), 25 mg vial	www.selleckchem.com	Cat# P1029
Trifluoroacetic acid	www.sigmaaldrich.com	Cat# T6508
Pierce phosphatase inhibitor cocktail	www.thermofisher.com	Cat# A32957
Pierce Protease Inhibitor cocktail	www.thermofisher.com	Cat# A32953
Methanol, ACS-grade LC reagent, ≥99.9%	www.sigmaaldrich.com	SKU# 439193
Acetonitrile, LC-MS LiChrosolv®	www.sigmaaldrich.com	SKU# 1000291000
Formic acid, ACS reagent, Ph. Eur., ≥98%	www.sigmaaldrich.com	SKU# 33015
Custom-synthesized stable isotope labeled Oxt (H2N-CYI^QNCPLG-amide; I^ = Isoleucine (13C6,15N)	www.vivitide.com	Ref# M197987 Rev 2
Critical commercial assays		
Oxytocin - Fluorescent EIA Kit	https://phoenixpeptide.com/	FEK-051-01
DetectX® Oxytocin ELISA Kit	www.arborassays.com	K048-H1
Subcellular Protein Fractionation Kit	www.thermofisher.com	Cat# 87790
Prometheus Protein Biology Products ProSignal® Dura ECL Reagent	https://geneseesci.com/	Cat # 20-301
Zymo Research EZ Methylation kit	www.zymoresearch.com	Cat# D5002
HotstarTaq DNA polymerase kit	www.qiagen.com	Cat# 203205
Custom designed assay for genomic DNA isolation	www.epigendx.com	Cat# ASY1570
Dynabeads® mRNA DIRECT™ Kit	www.thermofisher.com	Cat# 610.12
SuperScript III RT enzyme	www.thermofisher.com	Cat# 18080093
NovaSeq 6000 Sequencing System	www.illumina.com	
Deposited data		
Raw RNA sequencing data and the count metrices	This paper	Gene Expression Omnibus (GEO) accession number GSE228913
Experimental models: Organisms/strains		
CD® (Sprague Dawley) Rats, 8-10 weeks old Female, Timed pregnant E14, strain-001	www.criver.com	CD IGS# 001
Oligonucleotides		
Custom TaqMan® OxtR probe- Rn00563503_m1	www.thermofisher.com	Cat# 4331182
Custom TaqMan® Actb probe- Rn00667869_m1	www.thermofisher.com	Cat# 4331182
Custom TaqMan® Pgk1 probe- Rn01474008_gH	www.thermofisher.com	Cat# 4331182
RNeasy mini kit (50)	www.qiagen.com	Cat# 74104
SuperScript™ IV VILO™ Master Mix	www.thermofisher.com	Cat# 11756050
TaqMan™ Fast Advanced Master Mix	www.thermofisher.com	Cat# 4444964
Applied Biosystems™ 7500 Real-Time PCR System	www.thermofisher.com	Cat# 4351104

Continued

REAGENT or RESOURCE	SOURCE	IDENTIFIER
Software and algorithms		
Image Studio Software	www.licor.com	V.5.2.5
iPRECIO management software (IMS-200)	www.alzet.com	IMS-200
Illumina DRAGEN Bio-IT server software	www.illumina.com	V.3.9.3-8
R/Bioconductor package EdgeR		Ref Robinson et al.[86]
R/Bioconductor package Limma		Ref Ritchie et al.[87]
Limma's voomWithQualityWeights		Ref Liu et al.[88]
R/Bioconductor package GAGE		Ref Luo et al.[89]
R/Bioconductor package heatmap3		Ref Zhao et al.[90]
KEGG graphs with the R/Bioconductor package Pathview		Ref Luo and Brouwer[91]
R/Bioconductor package WGCNA		Ref Langfelder and Horvath[92]
R/Bioconductor package clusterProfiler		Ref Yu et al.[93]
Prism 9 for macOS	GraphPad Software Inc.	V.9.4.1
IBM SPSS Statistics		V.28
MATLAB	https://www.mathworks.com/products/matlab.html	Ref Hakon et al.[94]
Illustrations	https://www.biorender.com/	
Waxholm Space Atlas of the Sprague Dawley Rat Brain	https://www.nitrc.org/projects/whs-sd-atlas	RRID:SCR_017124
Other		
Micro infusion pump iPRECIO®	www.alzet.com	SMP-200
Bullet Blender	www.nextadvance.com	Storm 24
Pierce™ Peptide Desalting Spin Columns	www.thermofisher.com	Ref# 89852
Tecan multi-detection microplate reader	www.tecan.com	Infinite M200 PRO
LI-COR Fc imaging system	www.licor.com	Odyssey Fc Imager
iPRECIO data communication device (IMS-200)	www.alzet.com	IMS-200
Pyrosequencing PSQ 96HS system	www.biotage.com	PSQ 96HS
Vanquish Horizon UHPLC equipped with Orbitrap Exploris™ 240	www.thermofisher.com	
Waters ACQUITY HSS T3 C18 column (2.1 x 150 mm, 1.8 μm)	www.waters.com	SKU# 186003540
Heated Electrospray Ionization (HESI-II) Probe	www.thermofisher.com	Cat#IQLAAEGABBFACNMAGY
Rodent brain matrix, 1 mm	www.tedpella.com	Cat# 15065

RESOURCE AVAILABILITY

Lead contact

Further information and requests for resources should be directed to the lead contact, Arvind Palanisamy (arvind.palanisamy@wustl.edu).

Materials availability

This study did not generate any unique reagents.

Data and code availability

The RNA sequencing data are available through Gene Expression Omnibus (GEO) under the accession number GSE228913 ('*Transcriptomic changes in the medial prefrontal cortex of juvenile rat offspring after induced birth with oxytocin*').

This paper does not use customized code and does not report original code.

Any additional information required to reanalyze the data reported in this paper is available from the lead contact upon request.

EXPERIMENTAL MODEL AND STUDY PARTICIPANT DETAILS

Labor induction with Oxt was performed in timed-pregnant CD® (Sprague Dawley) IGS rat (Crl:CD[SD] outbred) as described previously.[38] Briefly, saline-primed iPrecio pump implantation was performed on gestational day (GD)16, followed by initiation of birth induction with Oxt on GD21. We focused on the direct effects of Oxt motivated by prior reports suggesting a direct effect on Oxtr in the developing brain,[31,47] and based on our data that excluded oxidative stress as a potential mechanism.[38] Experiments were performed in multiple cohorts over a 3-year period (Table S1). All animal experiments and methods reported here were approved by the Institutional Animal Care and Use Committee at Washington University in St. Louis (#20170010) and conducted in compliance with institutional and ARRIVE guidelines (Supplemental File).

METHOD DETAILS

Pup retrieval test

To determine whether Oxt-exposed postpartum mothers could positively respond to pup separation, we performed the pup retrieval test. Briefly, on postnatal day P2, pups were separated from their respective mothers for 10 min and placed in a 35°C heated cup. Three randomly chosen pups of either sex were subsequently placed in the three corners of the cage with their biological mother (either Oxt-exposed or unexposed). We measured: (i) the latency to retrieve the first pup, (ii) total time to retrieve all 3 pups, and (iii) the efficacy of retrieval in 5 min (for example, if all 3 pups were retrieved to the nest within 5 min, efficacy was 100%).

Qualitative assessment of maternal nurturing behavior

To ensure that the Oxt-exposed dam did not exhibit abnormal maternal behavior, we performed two 30-min video recordings 5-6 h apart, to examine the interaction between the mother and her pups (60 min total assessment time) over two days (P5-6). Recorded videos were scored to determine the total duration of maternal (licking, grooming, nest building, active or passive nursing) and nonmaternal behaviors (maternal self-care behaviors such as eating, drinking and self-grooming, or pups out of the nest) as described by Lee et al.,[95] and reported as a percentage of the total observation time.

Licking and grooming 'pen mark' assay

We quantified the extent of maternal licking and grooming of pups with the pen mark assay on P7 as described by Lee et al.[95] Briefly, we marked the top of the head and the bottom of the torso on the dorsal side of the pups with a laboratory marker and returned the pups to their mothers in home cages for 24 h. Next day, we assessed the quality of the marks based on an arbitrary scoring system: 0, no visible mark (implying excellent licking and grooming); 1, extremely faint mark; 2, clearly visible but faint mark; and 3, fully visible mark (implying poor licking and grooming). The average of the two scores (for head and body each) was calculated for each pup, averaged per dam, and subsequently compared between Con and Oxt groups.

Weigh-suckle-weigh (WSW) method to assess milk intake

We assessed milk intake of P12 pups with the WSW method. These experiments were performed between 13:00 and 17:00 h. Briefly, pups were separated from their mothers and grouped in dedicated pipette tip boxes containing appropriate cage bedding. The ambient temperature surrounding these boxes was maintained at approximately 30°C with radiant heating. After a 3 h separation, pups from the same litter were collectively weighed (pre-feeding weight) and returned to their respective mothers for a 1 h nursing bout following which they were immediately weighed again (post-feeding weight). The difference between the post- and pre-feeding weights was considered a surrogate measure of milk intake and was normalized to the litter size and expressed as milk intake/pup (mL).

Quantification of Oxt in the fetal plasma and brain

We performed Oxt quantitation in the fetal plasma and brain samples collected during our recent study.[38] Briefly, fetal blood was collected from at least 6 pups extracted by cesarean delivery 8-12 h after either labor induction with Oxt or unmanipulated labor as described by us previously.[96] All fetal blood samples collected from pups from the same dam were pooled as one unit. Collected samples were centrifuged at 1500 g for 10 min at 4°C, and plasma was stored at -80°C. During these experiments, we also collected the brains from pups. Cortical hemispheres from one fetal brain/dam were homogenized in a bullet blender (Next Advance, Inc.) and dissolved in PBS containing protease and phosphatase inhibitor cocktail at 4°C. Samples were then incubated at 100°C for 10 min for complete inhibition of proteases followed by chilling on ice for 2 min. Trifluoroacetic acid (1% TFA) was added to extract peptides on ultrasonic bath (Branson 1510) for 1 min. Tissue debris was removed by centrifugation at 14000 x g for 30 min at 4°C. Both plasma and brain homogenate were C-18 extracted, lyophilized, and assayed for Oxt in duplicate using a fluorescent enzyme immunoassay kit (#FEK-051-01, Phoenix Pharmaceuticals, Inc.). Oxt levels, normalized to total protein concentration, were compared between Oxt and control conditions.

Stable isotope labeled Oxt (SIL-Oxt) for assessment of placental transfer

Because exogenous Oxt is indistinguishable from endogenous Oxt, we performed additional experiments with custom-synthesized stable isotope labeled Oxt ([13C,15N]-Ile labeled Oxt; SIL-Oxt, Vivitide Inc.) to ascertain placental transfer. Briefly, extracted metabolites from

maternal and newborn plasma samples from SIL-Oxt treated GD21 dams (administered through iPrecio pump using the same protocol as that for Oxt; 100 mcg/mL) were resuspended with 30 µL of 50% MeOH and centrifuged to avoid debris prior to injection for LC-MS/MS on a Vanquish Horizon UHPLC equipped with Orbitrap Exploris™ 240 (Thermo Scientific). The samples were injected onto Waters ACQUITY HSS T3 C18 column (2.1 x 150 mm, 1.8 µm) and eluted at a flow rate of 400 µL/min with 2% mobile phase B (90% acetonitrile with 0.1% formic acid) for 2 min, followed by a linear gradient to 27% for 7 min, 98% for 7 min then held 2 min with 2% mobile phase A (0.1% formic acid in water) over 22 min gradient. Analyses were carried out using Heated Electrospray Ionization (HESI-II) Probe in the positive ion mode. For the full MS scan mode, precursor ion was isolated by quadrupole in 1.6 m/z window and analyzed in Orbitrap at 60,000 resolution. The SIL-Oxt was detected at a precursor mass of 1014.46 m/z. For the parallel reaction monitoring (PRM) of SIL-Oxt, fragment ions were scanned using Orbitrap at 15,000 resolution and the collision energy was optimized at 27% by stepwise increment. The MS2 ion spectra were acquired within a time window from 9.30 to 10.15 min. The following instrument settings were optimized for the PRM: isolation window, 1.0 m/z; RF Lens level 30%; AGC target, 2e5; and Maximum injection time, 200 ms. For the quantification of SIL-Oxt, the most intense and quantifiable MS2 ion, 730.28 m/z, was selected by the linearity test using a calibration curve. Each calibration point was analyzed in triplicate and the linear range was determined by the maximum number of points that could be included for the R^2 to remain > 0.99 and the coefficient of variation (CV) to be < 20% in triplicates. The lower limit of quantitation (LLOQ) was determined by the lowest value on the linear range which is higher than limit of detection (LOD) defined by 3 sigma of blank signal. The calibration range was 254 pg/mL to 1 µg/mL (R^2 = 0.9991) and the LOD was 127 pg/mL. The concentration of exogenous SIL-Oxt was calculated by 1/x weighted linear regression and the LOD was taken as the y-intercept for calculation. SIL-Oxt detection and quantification was performed at the Mass Spectrometry Technology Access Center (MTAC) at Washington University.

Evaluation of OxtR gene and protein expression in the brain

Similar methods were employed for Oxtr gene expression studies in the cortex of P1 pups and in bilaterally dissected mPFC and BLA tissue, and the hypothalamus from male and female P40 pups. Western blot was done as described for OxtR expression in the uterine myometrium,[38] except that membrane-associated proteins were isolated from the fetal cortex, using Subcellular Protein Fractionation Kit (catalog 87790; Thermo Fisher Scientific) following manufacturer's instructions. Immunoblots were incubated with ProSignal® Dura ECL Reagent (catalog #20-301, Prometheus Protein Biology Products) for 1 min at room temperature and detection of bound antibody was achieved with LI-COR Fc imaging system (LI-COR Biosciences Inc.).

DNA methylation analysis of the OxtR promoter region

We probed the DNA methylation status of 7 CpG sites in the promoter region of the Oxtr gene (from ATG -1349 to -1295, from TSS -1319 to -1265, Rnor_6.0/rn6 Chr#4 144417435-144417381, amplicon size:120 bp). Briefly, 200 - 500 ng of genomic DNA isolated from the frontal cortex of Oxt or saline-exposed pups was subjected to bisulfite modification with Zymo Research EZ Methylation kit (cat. # D5002, Zymo Research, Irvine, CA). HotstarTaq DNA polymerase kit (cat. # 203205, Qiagen, Inc.) was used to amplify the Oxtr target region using forward and reverse primer set with the following PCR conditions: 15 min at 95°C, 45 cycles of 95°C for 30s, 51°C for 30s, and 68°C for 30s, and a 5 min 68°C extension step. Pyrosequencing was performed with the PSQ 96HS system (Qiagen) as described by Beery et al.[97] with modifications. DNA methylation analysis after the genomic DNA isolation step was performed by EpigenDx (Hopkinton, MA) using a custom designed assay (ASY1570).

Oxt plasma assays at P40

We performed plasma Oxt quantitation in P40 pups. Briefly, under isoflurane anesthesia 1 mL of blood was directly aspirated from the left ventricle using a 21G needle, mixed in a BD Vacutainer EDTA tube, and subsequently centrifuged at 1500 g for 10 min at 4°C. Approximately 500-600 µL of plasma was stored at -80°C. Samples were assayed for Oxt using an enzyme immunoassay kit (#K048-H1, Arbor Assays, Inc.) according to manufacturer's instructions. In brief, each sample was diluted 1:8 in the assay buffer and applied to the designated well(s), respectively. All experiments were performed in duplicate, and the absorbance was read with Tecan Infinite M200 PRO (Tecan Group Ltd., Switzerland) at 450 nm. Oxt concentrations were determined by comparison with predetermined standards, corrected for the dilution factor and reported as pg/mL.

Assessment of behavioral phenotype after Oxt-induced birth

Rat pups were assessed for behavioral consequences of Oxt-induced birth at P8 and again through juvenility and adolescence. For all tasks, the rats were acclimated to the testing room at least 30 min prior to the start of testing. All assays were conducted by experimenters blinded to experimental group designations during testing, which occurred during the light phase. The order of behavioral tests was chosen to minimize the effects of stress on performance. To minimize any effect of hormonal cycling during the peripubertal period, behavior testing across experimental groups were conducted at the same time of day to control for variation in testosterone levels across the day in males or other circadian effects. Likewise, in females, status of vaginal openings as a proxy for estrous phase were monitored during behavior testing. Unexposed and Oxt-exposed offspring of both sexes were assessed for early communicative behavior with maternal isolation-induced ultrasonic vocalizations (USV), anxiety-like behaviors with elevated plus maze, social behaviors with social investigation and social play, cognitive inflexibility with spontaneous alternations, sensorimotor gating with prepulse inhibition, and empathy-like behaviors with observational fear learning.

Maternal isolation-induced ultrasonic vocalizations

Maternal isolation-induced ultrasonic vocalizations (USVs) produced by the pup is one of the earliest forms of social communication we can examine in the rat, and these isolation calls elicit maternal care from the dam.[98,99] USVs were recorded on P8 following our methods adapted for the rat from our previous publication.[100] Briefly, the dam was removed from the nest and the litter was placed on a heating pad to maintain body temperature while away from the dam. The surface temperature of each pup was recorded (HDE Infrared Thermometer; Saline-exposed: M=35.3°C, SD=0.54; Oxt-exposed: M=35.2°C, SD=0.69) prior to placement in an empty polycarbonate cage (28.5 cm x 17.5 cm x 12 cm) in a sound-attenuating chamber (Med Associates Inc., Fairfax, VT). USVs were recorded for three minutes using an Avisoft UltraSoundGate CM16 microphone, Avisoft UltraSoundGate 116H amplifier, and Avisoft Recorder software (gain = 8.5 dB, 16 bits, sampling rate = 250 kHz). The pup was then weighed and returned to the nest. The dam was returned to the nest following recording of the last pup in the litter. Individual syllables and other temporal and spectral features were extracted from the waveform audio files using the Avisoft-SASLab Pro Sound Analysis Software (frequency range = 25 kHz to 120 kHz, FFT size = 512, overlap = 50%, time resolution = 1.024 ms, frequency resolution = 488.2 Hz).

Elevated plus maze

Passive avoidance behavior for an open, elevated area was assessed in the elevated plus maze on P26 as previously published.[56] Briefly, each rat received one five-minute trial conducted in a dark room. The elevated (62.5 cm) apparatus was made of opaque acrylic and comprised two enclosed arms, two open arms (36 cm x 6.1 cm x 15 cm each), and a center platform (5.5 cm x 5.5 cm). Movement within the apparatus was quantified via breaks in photobeam pairs. Percent time in the open arm and total distance traveled were analyzed. The apparatus was cleaned with 0.02% chlorhexidine diacetate solution between animals.

Juvenile social play

Social interactive behaviors were measured at P28 in dyadic, sex- and treatment-matched pairings adapted from previous methods.[101] To potentiate social behaviors, each rat was isolation housed for two and one-half hours prior to recordings and paired with a non-cage mate during testing. Rats were placed in an open field (40 cm x 40 cm x 40 cm) with opaque walls under white lighting (315 lux) and recorded for ten minutes via Any-maze tracking software (Stoelting, Co.). The apparatus was cleaned with 0.02% chlorhexidine diacetate solution between animals. Play behaviors such as pouncing, pinning, boxing and chasing were not observed. Therefore, additional social interaction behaviors, including sniffing, allogrooming and following, were scored manually by a blinded experimenter. A composite score of all three behaviors was calculated for frequency, duration, and mean bout duration, as well as latency to first behavior.

Spontaneous alternation Y-maze

To assess spatial working memory and cognitive inflexibility in behavioral patterns, we used the spontaneous alternation Y-maze at P30 based on previous methods.[101–103] Briefly, each rat was placed in the center of a Y shaped maze made of black acrylic under dim white lighting (8.5 lux) and allowed to freely explore for 8 minutes. Each arm measured 40 cm x 10 cm x 20 cm. Any-maze tracking software was used to quantify the spontaneous alternations, which were defined as any three consecutive choices of three different arms without re-exploration of a previously visited arm. The percentage of alternations was determined by dividing the total number of alternations by the total number of choices minus two. The apparatus was cleaned with 0.02% chlorhexidine diacetate solution between animals.

Juvenile dyad USVs

Communication behavior was assessed at P34 by measuring USVs emitted during dyadic, sex- and treatment-matched interactions. To potentiate vocalizations, each rat was isolation housed for two and one-half hours prior to recordings and paired with a non-cage mate during recordings. For ten minutes, the rat pair was placed in an empty chamber (47.6 cm × 25.4 cm × 20.6 cm) inside a sound attenuating chamber (Med Associates Inc, Fairfax, VT). The chamber was cleaned with 0.02% chlorhexidine diacetate solution between animals. USVs were recorded as described above for maternal isolation-induced pup USVs. Data were analyzed at the level of dyad.

Acoustic startle/prepulse inhibition

Sensorimotor gating and startle reflex were assessed at P41 in the acoustic startle/prepulse inhibition (PPI) test as previously described.[100] Briefly, each rat received one test session during which acoustic startle to a 120 dB auditory stimulus pulse (40 ms broadband burst) and PPI (response to a startle pulse following a prepulse 100 ms earlier) were measured on a force plate apparatus using computerized instrumentation (StartleMonitor, Kinder Scientific). During the 20 min test, a total of 65 trials were presented including non-startle trials during the first 5 min, which served as an acclimation period when no stimuli above the 65 dB white noise background were presented. Startle reflex was measured across twenty startle trials. The first and second to last set of trials included 5 consecutive startle (120 dB pulse alone) trials unaccompanied by other trial types. The middle 10 startle trials were interspersed with PPI trials, consisting of an additional 30 presentations of 120 dB startle stimuli preceded by prepulse stimuli of 4, 12, or 20 dB above background (10 trials for each PPI trial type). A percent PPI score for each trial was calculated using the following equation: %PPI = 100 × (startle pulse alone − prepulse + startle pulse)/startle pulse alone. The final 5 trials included startle trials with the stimulus increasing from 80 to 120 dB as a measure of startle sensitivity. The apparatus was cleaned with 0.02% chlorhexidine diacetate solution.

Social approach

Sociability was assessed at P43 in the 3-chambered apparatus social approach task following our previously published methods.[56] Briefly, each rat received two consecutive, ten-minute trials in a three chambered apparatus (100 cm x 100 cm x 22 cm). The first trial served to habituate the animal to the apparatus including the stimulus withholding cylinder, while the second trial measured sociability, or the tendency to initiate social contact with a novel sex-, strain- and age-matched conspecific rat sequestered in the withholding cylinder. The duration investigating within 2cm of each cylinder (stimulus and empty), time and entries into each chamber, and total distance traveled were quantified. The apparatus was cleaned 0.02% chlorhexidine diacetate solution and the withholding cylinders with 70% ethanol between animals.

Observational fear learning

To assess empathy-like fear responses, we conducted the observational fear learning (OFL) assay at P48-49 as previously described.[56] Briefly, rats were conditioned to context-dependent fear by observing an age-, strain- and sex-matched conspecific receive foot shocks. The apparatus (27 cm x 31 cm x 30.5 cm) consisted of an acrylic chamber divided by a transparent acrylic wall with 90 equidistant 1cm-diameter holes to allow for scent and sound penetration. The stimulus rat was sequestered to one half of the cage on a stainless-steel grid floor that allowed for the presentation of 1.0 mA foot shocks. The observer side of the chamber was fitted with an opaque acrylic floor to prevent the animal from receiving foot shocks. On day one, the first five minutes served as acclimation to the apparatus and to record baseline freezing behaviors. During the second 4 minutes, the stimulus rat received a 1.0 mA foot shock every 10 s. The freezing behavior of the observer rat was measured. On day 2, the observer rat was placed back in the apparatus without the stimulus rat or foot shocks, and freezing behavior was quantified as a measurement of observational fear memory during the nine-minute test session. The apparatus was cleaned 0.02% chlorhexidine diacetate solution between animals.

Assessment of puberty onset

Male and female offspring (n=3 each from 3 independent litters unexposed or exposed to Oxt) were monitored daily from P28 through P40 to determine the day of onset of puberty with balano-preputial separation and vaginal opening, respectively.[104] In addition, we performed vaginal cytology experiments in female offspring to confirm onset of puberty with establishment of the estrus cycle.[105] Body weights were simultaneously measured at multiple timepoints to track somatic growth of the offspring.

RNA-seq to assess the impact of Oxt on the medial prefrontal cortex transcriptome

Motivated by sex-specific neurobehavioral changes implicating the medial prefrontal cortex (mPFC), we performed RNA-seq to assess the mPFC transcriptome in postnatal day P45 male and female control and Oxt-exposed offspring to facilitate correlation with behavioral studies. Briefly, we isolated the mPFC after sectioning the brain in the coronal plane (1 mm) using a rodent brain matrix (Ted Pella Inc.) with atlas-based anatomic guidance (Paxinos & Watson, 6th edition). Total RNA was extracted using RNAeasy kit (Qiagen) and subjected to RNA-seq (Genome Technology Access Center core facility). Only RNA with RIN > 8.0 were used for RNA-seq. Library preparation was performed with 5 to 10ug of total RNA with a Bioanalyzer RIN score greater than 8.0. Ribosomal RNA was removed by poly-A selection using Oligo-dT beads (mRNA Direct kit, Life Technologies). mRNA was then fragmented in reverse transcriptase buffer and heating to 94 degrees for 8 minutes. mRNA was reverse transcribed to yield cDNA using SuperScript III RT enzyme (Life Technologies, per manufacturer's instructions) and random hexamers. A second strand reaction was performed to yield ds-cDNA. cDNA was blunt ended, had an A base added to the 3' ends, and then had Illumina sequencing adapters ligated to the ends. Ligated fragments were then amplified for 12-15 cycles using primers incorporating unique dual index tags. Fragments were sequenced on an Illumina NovaSeq-6000 using paired end reads extending 150 bases. RNA-seq reads were then aligned and quantitated to the Ensembl release 101 primary assembly with an Illumina DRAGEN Bio-IT server running version 3.9.3-8 software.

All gene counts were then imported into the R/Bioconductor package EdgeR[86] and TMM normalization size factors were calculated to adjust for differences in library size between samples. Ribosomal genes and genes not expressed in the smallest group size minus one samples greater than one count-per-million were excluded from further analysis. The TMM size factors and the matrix of counts were then imported into the R/Bioconductor package Limma.[87] Weighted likelihoods based on the observed mean-variance relationship of every gene and sample were then calculated for all samples and the count matrix was transformed to moderated log 2 counts-per-million with Limma's voomWithQualityWeights.[88] The performance of all genes was assessed with plots of the residual standard deviation of every gene to their average log-count with a robustly fitted trend line of the residuals. Differential expression analysis was then performed to analyze for differences between conditions and the results were filtered for only those genes with Benjamini-Hochberg false-discovery rate adjusted p-values less than or equal to 0.05. For each contrast extracted with Limma, global perturbations in known Gene Ontology (GO) terms, MSigDb, and KEGG pathways were detected using the R/Bioconductor package GAGE[89] to test for changes in expression of the reported log 2 fold-changes reported by Limma in each term versus the background log 2 fold-changes of all genes found outside the respective term. The R/Bioconductor package heatmap3[90] was used to display heatmaps across groups of samples for each GO or MSigDb term with a Benjamini-Hochberg false-discovery rate adjusted p-value less than or equal to 0.05. Perturbed KEGG pathways where the observed log 2 fold-changes of genes within the term were significantly perturbed in a single-direction versus background or in any direction compared to other genes within a given term with p-values less than or equal to 0.05 were rendered as annotated KEGG graphs with the R/Bioconductor package Pathview.[91]

To find the most critical genes, the Limma voomWithQualityWeights transformed log 2 counts-per-million expression data were then analyzed via weighted gene correlation network analysis with the R/Bioconductor package WGCNA.[92] Briefly, all genes were correlated across each other by Pearson correlations and clustered by expression similarity into unsigned modules using a power threshold empirically determined from the data. An eigengene was then created for each *de novo* cluster and its expression profile was then correlated across all coefficients of the model matrix. Because these clusters of genes were created by expression profile rather than known functional similarity, the clustered modules were given the names of random colors where grey is the only module that has any pre-existing definition of containing genes that do not cluster well with others. These *de novo* clustered genes were then tested for functional enrichment of known GO terms with hypergeometric tests available in the R/Bioconductor package clusterProfiler.[93] Significant terms with Benjamini-Hochberg adjusted p-values less than 0.05 were then collapsed by similarity into clusterProfiler category network plots to display the most significant terms for each module of hub genes in order to interpolate the function of each significant module. The information for all clustered genes for each module were then combined with their respective statistical significance results from Limma to determine whether or not those features were also found to be significantly differentially expressed.

Functional connectivity mapping with optical intrinsic signal imaging

Functional connectivity of the brain of OXT and saline-exposed male offspring was assessed at P23 using a reflectance-mode functional connectivity optical intrinsic signal imaging (fcOISI) system.[106] The fcOISI system images the brain through the intact skull and records spontaneous fluctuations in oxy- and deoxyhemoglobin. Through neurovascular coupling, these fluctuations represent spatiotemporal variations in neural activity, similar to human BOLD-fMRI. Briefly, juvenile rats were anesthetized with an i.p. injection of ketamine (86.9 mg/kg) and xylazine (13.4 mg/kg) as described previously.[107] Optical intrinsic signals were acquired during sequential elimination provided by four polarized light emitting diodes (LEDs, Thorlabs, 470 nm: M470L3-C1, 590 nm: M590L3-C1, 617 nm: M617L3-C1, and a 625 nm: M625L3-C1) placed approximately 20 cm above the rat's head. Diffuse reflected light from the rat head was detected by a cooled, frame-transfer EMCCD camera (iXon 897 Ultra, Andor Technologies). A crossed linear polarizer was placed in front of the camera lens to reject specular reflection from the LEDs. The LEDs and camera were time-synchronized and controlled via a National Instruments data Acquisition card (NI PCI 6733) and computer (Dell Workstation) using custom-written software (MATLAB, Mathworks) at a frame rate of 120 Hz (30 Hz/LED). Image processing and functional connectivity measurements (including seed-based functional connectivity and regional node degree) were performed as described previously by our group.[94] Briefly, seeds for functional connectivity analysis were placed in cortical areas corresponding to frontal, cingulate, motor, somatosensory (SS), retrosplenial, visual and auditory networks. From each seed region, time traces of oxygenated hemoglobin were correlated with time courses in all brain pixels, generating a resting state-functional connectivity (RS-FC) map for each seed. Individual rat pup RS-FC maps were transformed to Fisher z-scores and averaged within each group. Seed-based RS-FC maps were displayed using a color scale where negative correlations were in blue hues and positive correlations in red hues. RS-FC matrices were constructed by compressing RS-FC maps to report RS-FC between each seed-seed pair. Correlating each pixel's time course with the time courses of all other pixels in the brain yields a matrix containing all of the RS-FC information within our field-of-view. Specifically, each row or column of this matrix represents a pixel's RS-FC map. The number of functional connections (degree) of each pixel (node) was determined by thresholding this matrix at $z(r) \geq 0.4$, so that only strong positive RS-FC contributed to each pixel's measure of node degree. Summing the correlation coefficients above this threshold over pixels in the same (ipsilateral) or opposite (contralateral) hemisphere relative to a candidate pixel produced a weighted measure of intra- or inter-hemispheric node degree for that pixel, respectively. This procedure was performed in each rat over pixels within the shared brain mask. Group-level maps were created by averaging intra- and inter-hemispheric node degree maps across rats, and quantified within brain regions.

Ex vivo DTI for structural connectivity assessment

MRI of fixed adult rat brains was performed on a Varian Agilent (Santa Clara, CA) 11.74 T DirectDrive MRI system. The rat brains were immersed in Fluorinert, and images were acquired at $125 \times 125 \times 500 \ \mu m^3$ resolution with a 192×192 matrix and 45 slices. T2-weighted spin echo anatomic images were acquired using TR = 2000 ms, TE = 20 ms, and 2 averages. Diffusion tensor images were acquired using TR = 2000 ms and TE = 25.5 ms over 26 combinations of b-value and diffusion directions, bmax = 3000 s/mm^2, δ = 5 ms, Δ = 15 ms. Brain regions of interest (mPFC, corpus callosum, amygdala) were identified by registering the T2-weighted MRI images to the Waxholm Space Atlas of the Sprague Dawley Rat Brain (https://www.nitrc.org/projects/whs-sd-atlas) using ANTs (Advanced Normalization Tools).[108] The brain regions were mapped onto the acquired MRI data through automated registration against a rat brain atlas. The resulting segmentations were imperfect, especially on brains where fixation and subsequent handling produced cracks or gross distortion in the external shape of the brain. While we manually adjusted the segmentations in particularly egregious cases, the lack of a trend across treatments or regions (except perhaps for the CC FA) strongly indicated that the results would not be affected by minor refinements to the region definitions. Diffusion tensor eigenvalues and parametric maps of apparent diffusion coefficient (ADC) and fractional anisotropy (FA) were calculated according to standard equations[109,110] using the Bayesian Toolbox,[111] a data modeling software package based upon Bayesian probability theory. Daxial and Dradial represent the first diffusion eigenvalue (along the direction of white-matter fibers) and the average of the second and third eigenvalues (perpendicular to the white-matter fibers), respectively.

QUANTIFICATION AND STATISTICAL ANALYSIS

Data outliers were detected and eliminated using ROUT (robust regression and outlier analysis) with Q set to 1%. Normality of residuals was checked with D'Agostino-Pearson omnibus test. For experiments where sex was not included as a variable, data were analyzed with either Welch's t-test or Mann-Whitney test as appropriate. Oxt dose-response data were analyzed with one-way ANOVA with Dunnett's test for multiple comparisons. Because of established sex differences in Oxtr expression and Oxt signaling at or around weaning, data from $\geq$ P21 pups were independently analyzed by sex. For analyses of behavioral data, we first screened for missing values and fit of distributions with assumptions underlying univariate analysis. This included the Shapiro-Wilk test on z-score-transformed data and qqplot investigations for normality, Levene's test for homogeneity of variance, and boxplot and z-score (± 3.29) investigation for identification of influential outliers. Means and standard errors were computed for each measure. Parametric models including student's t-test and analysis of variance (ANOVA), including one-way, factorial and repeated measures, were used to analyze data where appropriate, and simple main effects were used to dissect significant interactions. Sex was included as a biological variable in all analyses. Where appropriate, the Greenhouse-Geisser or Huynh-Feldt adjustment was used to protect against violations of sphericity for repeated measures designs. Multiple pairwise comparisons were subjected to Bonferroni correction, where appropriate. For data that did not fit univariate assumptions, non-parametric tests were used, or data transformations were applied. The critical alpha value for all behavioral analyses was $p \leq 0.05$ unless otherwise stated. RNA-seq data were analyzed with generalized linear models to test for gene/transcript level differential expression between conditions and the results were filtered for only those genes with Benjamini-Hochberg false-discovery rate adjusted p-values (FDR) ≤ 0.05. Perturbations in known Gene Ontology (GO) terms and KEGG pathways were detected using the R/Bioconductor package GAGE to test for changes in expression of the reported log 2 fold-changes reported by Limma in each term versus the background log 2 fold-changes of all genes found outside the respective term. GO terms were considered significant with FDR ≤ 0.05 and KEGG terms were marked as significant with p-values $\leq$ 0.05. Prior to statistical testing of fcOISI measures, Pearson r values were transformed to Fisher z-scores. Maps of node degree were compared at each pixel using a two-tailed student's t-test assuming unequal group variance and corrected for multiple comparisons using clustering statistics. Quantitative DTI data for brain regions of interest were independently analyzed with either Welch's t-test or Mann-Whitney test as appropriate. Differences between groups were considered statistically significant if $p < 0.05$ following correction for multiple comparisons when necessary. Data are presented as mean $\pm$ SEM. Quantitative data were analyzed with Prism 9 for macOS (version 9.4.1; GraphPad Software Inc.), behavioral data were analyzed with IBM SPSS Statistics (v.28), and fcOISI data with MATLAB.